Marine Biology (2026) 173:38
https://doi.org/10.1007/s00227-025-04775-5

ORIGINAL PAPER

Heat stress alters the microenvironment of corals: oxygen depletion and oxidative damage in the gastrovascular cavity of two tropical species

Verdiana Vellani[1,2] · Walter Dellisanti[3] · Qingfeng Zhang[3] · Enrico Montalbetti[4,5,6] · Gregorio Motta[7] · Davide Seveso[4,5,6] · Monia Renzi[1,2] · Michael Kühl[3]

Received: 11 September 2025 / Accepted: 26 November 2025

Abstract

Current climate changes cause increasing stress to corals, which can disrupt host-symbiont relationships, leading to bleaching and mortality. While stress responses are well-documented at the coral colony and reef scales, less is known about how stress responses affect different compartments within the coral holobiont. Here, we investigated the impact of thermal stress on macro– and microscale compartments, including the endoderm-lined gastrovascular cavity (GVC) and the ectoderm-lined external tissue surface, in two tropical corals, *Caulastrea curvata* and *Galaxea fascicularis*. We assessed the coral physiological status via respirometry, variable chlorophyll fluorometry, O_2 and H_2O_2 microsensor analyses, chlorophyll measurements, and oxidative stress biomarkers during a 14-day thermal stress exposure. Under heat stress, both species showed a reduced O_2 concentration in the GVC by up to 90% in the light, reaching hypoxic (<50 µmol O_2 L^{-1}) to anoxic levels, while the O_2 concentration in the external surface tissue of *C. curvata* decreased by 20%. Moreover, no changes in the H_2O_2 dynamics of the coral's external tissue surface were detected. Lipid peroxidation in the gastrodermis of both species increased significantly by 90–198% indicating oxidative damage, although antioxidant enzyme activity (SOD and CAT), chlorophyll content, and bulk metabolic rates (respiration and photosynthesis) remained stable. Our findings indicated that thermal stress could affect the microenvironment of corals, particularly in the GVC, without visible bleaching or major disruptions in bulk physiology. This suggested the importance of microenvironmental metrics for the early detection of coral physiological stress.

Keywords Tropical corals · Heat stress · Microecology · Gastrovascular cavity · Biomarkers

Responsible Editor: C. Voolstra.

✉ Verdiana Vellani
verdiana.vellani@phd.units.it

✉ Monia Renzi
mrenzi@units.it

[1] Department of Life Sciences, University of Trieste, 34127 Trieste, Italy

[2] Consorzio Nazionale Interuniversitario Per Le Scienze del Mare (CoNISMa), 00196 Rome, Italy

[3] Department of Biology, Marine Biology Section, University of Copenhagen, 3000 Helsingør, Denmark

[4] Department of Earth and Environmental Sciences, University of Milano-Bicocca, 20126 Milan, Italy

[5] MaRHE Center (Marine Research and High Education Centre), Magoodhoo Island, Faafu Atoll, Maldives

[6] NBFC (National Biodiversity Future Center), 90133 Palermo, Italy

[7] Department of Integrative Marine Ecology, Stazione Zoologica "Anton Dohrn", 80121 Naples, Italy

Published online: 03 February 2026

Introduction

Coral reefs are hotspots of marine productivity and biodiversity (Duarte 2000; Knowlton et al. 2010; Wagner et al. 2020; Sobha et al. 2023), providing crucial ecosystem services such as supporting fisheries that sustain coastal communities, cultural services such as recreation and tourism, and coastal protection (Woodhead et al. 2019). Scleractinian corals harbor endosymbiotic dinoflagellate algae of the family Symbiodiniaceae (LaJeunesse et al. 2018) in their endoderm tissue (gastrodermis), which are essential in providing organic carbon and oxygen to the animal host (Stanley and Swart 1995). Together with their associated microbiota (bacteria, archaea, fungi, protists, and viruses), corals form a complex biological unit known as the coral holobiont, which underpins reef formation and resilience (Rohwer et al. 2002; Knowlton and Rohwer 2003; Rosenberg et al. 2007; van Oppen and Medina 2020; Goulet et al. 2020; Apprill 2025). However, this symbiosis is threatened by the ongoing climate change. Rising sea temperatures are among the most pervasive stressors to coral reefs, triggering coral bleaching events and eventually widespread coral mortality (Leggat et al. 2019; van Woesik et al. 2022). End-of-century temperatures are projected to rise 1–3 °C (or more) in tropical seawater (Pachauri et al. 2014), and mortality events are expected to occur with higher frequency in the next decades (van Hooidonk et al. 2014; Sully et al. 2022; Mellin et al. 2024).

A key player in the coral stress response is the overproduction of reactive oxygen species (ROS), which is crucially involved in coral cellular damage during heat stress (Downs et al. 2002; Weis 2008; Lesser 2011; Szabó et al. 2020; Isa et al. 2024). ROS species such as singlet oxygen ($^1O_2$), superoxide anion ($O_2^{\bullet-}$), and hydrogen peroxide (H_2O_2) are typically produced as byproducts of photosynthesis in the algal symbionts, and their production is proportional to the oxygen concentration in the tissue (Lesser 2006, 2011; Foyer and Hanke 2022). ROS can also be released by microbes and other organisms associated with the microbiome, as well as by cellular processes in the animal host (Hansel and Diaz 2021). While ROS serve essential signaling roles, their accumulation under thermal stress can increase antioxidant defenses, such as superoxide dismutase (SOD) and catalase (CAT), leading to oxidative damage and cellular dysfunction (Liñán-Cabello et al. 2010; Dias et al. 2019a, 2019b, 2020; Marangoni et al. 2021; Montalbetti et al. 2021; Isa et al. 2024). However, the precise mechanisms triggering oxidative stress and thermal sensitivity still remain debated (Oakley and Davy 2018; Helgoe et al. 2024). Lipid peroxidation (LPO) is a key marker of oxidative damage and increases when antioxidant systems are impaired or overwhelmed (Gaschler and Stockwell 2017). However, direct in vivo measurements of ROS remain technically challenging, and most studies rely on endpoint biochemical biomarkers or infer oxidative stress from bleaching severity and photosynthetic efficiency (Monserrat et al. 2007; Baird et al. 2009). Recently, the use of H_2O_2 and O_2 microsensors has also been introduced in laboratory studies of ROS dynamics in heat-stressed corals (Schlotheuber et al. 2024).

To date, the majority of studies of coral oxidative stress have been conducted at the holobiont level (van Oppen and Raina 2023), using sampling and analysis methods that average stress responses across the different compartments, i.e., mucus, tissue, and the coral skeleton that harbor different microbiomes and thus may exhibit different stress responses. Yet, corals are structurally complex, and their compartments can host markedly varying physical and biochemical conditions. In particular, the gastrovascular cavity (GVC) of the coral polyp constitutes a gastrodermis-lined central compartment for important functions in the coral holobiont, such as uptake and digestion of particulate materials, as well as the entry and exit path for Symbiodiniaceae during symbiont acquisition and expulsion, respectively (Hughes et al. 2022). The coral GVC can host a specific gut-like microbiome (Bollati et al. 2024) and exhibits peculiar chemical characteristics, such as a lower pH, different oxygen concentrations, and higher concentrations of Vitamin B12 and nutrients compared to the water surrounding the polyp (Agostini et al. 2012; Jokic et al. 2012; Bove et al. 2020; Hughes et al. 2022). Few studies have investigated the microenvironment and microbiome of the coral GVC (see Bollati et al. 2024), and so far, no studies have been conducted on the effects of increased temperature on the coral GVC microenvironment. In addition to the GVC, the external diffusive boundary layer (DBL) represents another key microenvironment in proximity to the external tissue surface, where biological activity can generate local gradients of chemical compounds (Shashar et al. 1993, 1996; Lesser et al. 1994; Kühl et al. 1995; Thomas and Atkinson 1997).

In this study, we investigated the thermal stress response of corals, focusing on both the macro– (polyp) and microscale (GVC and external tissue surface) levels of two tropical, reef-building corals, *Galaxea fascicularis* (Linnaeus, 1767) and *Caulastrea curvata* (Wijsman-Best 1972). We employed a multi-parametric approach including O_2 and H_2O_2 microsensors, variable chlorophyll fluorescence, chlorophyll quantification, and oxidative stress biomarkers (SOD, CAT, and LPO) over a 14-day heat stress exposure. Our findings highlight the potential of using microenvironmental diagnostics, especially GVC oxygen dynamics, as sensitive early indicators of coral stress.

Materials and methods

Coral husbandry

Colonies of the tropical scleractinian coral species *Galaxea fascicularis* and *Caulastrea curvata* (Fig. S1; 4 colonies per species) were obtained from Dejong Marine Life (Netherlands) in March 2024 and kept in the laboratory at the Marine Biological Section coral husbandry facilities in Helsingør (Denmark). *G. fascicularis* was selected as a well-established model species with documented microscale features, particularly within the GVC (Agostini et al. 2012; Bove et al. 2020; Puntin et al. 2023; Bollati et al. 2024), while *C. curvata*, a commonly used species in aquariology, was included due to the significant polyp size and its applicability to microsensors, as well as to explore micro-ecological responses in a non-model coral. Coral colonies were fragmented using a hammer and chisel, and the nubbins (n = 25 for *C. curvata*, n = 51 for *G. fascicularis*) were glued to the ceramic supports with GROTECH® Corafix SuperFast Epoxy and labeled. The nubbins were acclimated for 2 weeks in a 40 L aquarium at a temperature of 25 °C and a salinity of 35 ppt under an incident photon irradiance (400–700 nm) of 150 µmol photons m^{-2} s^{-1} (12 h:12 h light:dark, Fluval Sea Marine 3.0 Nano LED Aquarium 20W), measured with a photon irradiance meter equipped with a spherical micro quantum sensor at the coral surface level (Universal Light Meter, ULM-500 and US-SQS/L, Heinz Walz, Effeltrich, Germany). Constant water flow was ensured by two aquarium pumps (Universal Aquarium Pumps 106 s 5w; Tunze). The parameters maintained during the experiment are consistent with those commonly used in laboratory studies of cultured coral species that were not sampled from the field. The used acclimation period is in line with previous studies, in which 7–12 days were generally considered adequate (Grottoli et al. 2021). The incident photon irradiance was chosen as it is sufficient for the survival and growth of *G. fascicularis* (Schutter et al. 2012) and has previously been used for this species (Cheng et al. 2024). Nubbins were fed with *Artemia* nauplii twice weekly, and one-third of the water was renewed twice weekly.

At the end of the acclimation period, the nubbins of both species were randomly and equally distributed in the four experimental tanks (8 L each), in which the conditions of light, water change, and flow were identical to those during the acclimation period. Two aquaria were used as controls, and two were used for the temperature increase to perform the experiment in duplicate. During the heat stress experiment, the temperature was raised from 25 °C to 29 °C over a week (until day 7), with a maximum increase of 1 °C per day. The highest temperature of 29 °C (±1 °C; see Table S1 for details on the temperatures recorded on days 0, 7, and 14) was then maintained for a week, until day 14. The chosen temperature ramp aligns with the moderate intensity and duration criteria outlined by Grottoli et al. (2021). The experimental design and the analyses performed are shown schematically in Fig. 1. Potential pseudoreplication was checked by using a Generalized Linear Mixed Model (GLMM) within each species per treatment (see paragraph '*2.7 Statistical analysis*').

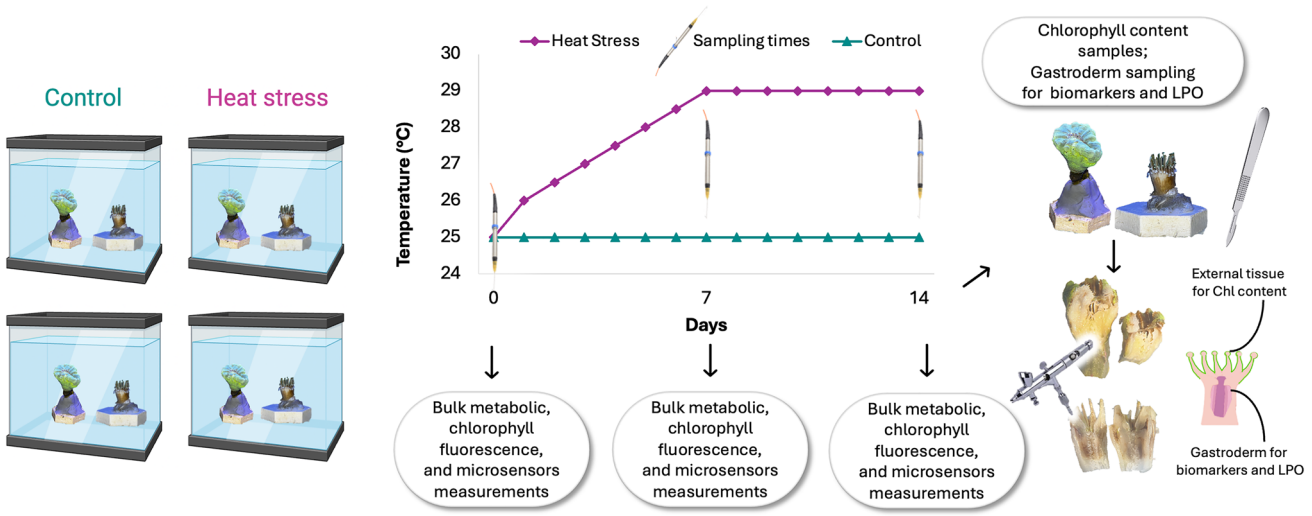

Fig. 1 Scheme summarizing the workflow and methodology used in the experiment. Two species of tropical coral (*C. curvata* and *G. fascicularis*) were subjected to two temperature treatments (in duplicate): a control (constant temperature at 25 °C) and a heat stress (temperature increased gradually from 25 °C to 29 °C over seven days, followed by maintenance at 29 °C until day 14). Coral physiological and microsensors measurements were performed at three time points: day 0, day 7, and day 14. These measurements included bulk metabolic, variable chlorophyll fluorescence, and microsensors measurements. Microsensor measurements involved the external tissue surface and the gastrovascular cavity (GVC). Additional analyses included chlorophyll content in external tissue and biochemical markers in gastrodermis

Bulk metabolic measurements

Coral photosynthesis and dark respiration were assessed on days 0, 7, and 14 (Fig. 1) during the exposure by measuring the net production or consumption of O_2 by corals incubated in custom-made, transparent, and gas-tight chambers (55 mL volume), as described by Dellisanti et al. (2024). The O_2 concentration in the chambers was monitored via O_2-sensitive optical sensor spots (OXSP5-ADH, Pyroscience GmbH) fixed inside each chamber. Each sensor spot was read out using a fiber optic cable (SPFIB-LNS, Pyroscience GmbH), which was connected to a fiber optic O_2 meter (FireSting-PRO, FSPRO-4, Pyroscience GmbH). The meter was connected via a USB cable to a PC running data logging software (Pyroscience Workbench V1.4.7.2305; Pyroscience GmbH). The sensors were calibrated before the start of the experiment in µmol O_2 L^{-1} using a two-point calibration method by measuring sensor signals in both anoxic (seawater deoxygenation with OXCAL Capsules; Pyroscience GmbH) and 100% air-saturated seawater at experimental temperature and salinity (25 °C and a salinity of 35). After a 10-min dark acclimation, O_2 in the chambers was recorded every second during incubations. During the experiment, the O_2 concentration values were temperature-compensated directly in the system operating software. Dark respiration (R) and net photosynthesis (P_{net}) were measured during 30-min dark and 30-min light incubations, respectively, aligning with widely adopted frameworks. The change in O_2 concentration over time in the chamber was calculated from the linear change of O_2 concentration during the incubation time using the '*respR'* package (Harianto et al. 2019) in the R software (R Core Team 2024). These rates were then multiplied by the volume of seawater surrounding the samples of coral in the chamber and divided by the surface area of the living part of the nubbin. The surface area of the living part of the coral was estimated using the cylindrical model technique in both species (Kahng et al. 2024). Gross photosynthesis (P_{gross}) rates were calculated by adding the absolute values of the respiration rates to P_{net}, assuming that dark respiration was representative of coral respiration in the light. The ratio of gross photosynthesis to respiration was then calculated as P_{gross}:R, which indicates the absolute value of respiration that occurs over 24 h, as described by Muscatine et al. (1981) and Coles and Jokiel (1977). Although it is recognized that respiration can vary significantly over diurnal and seasonal patterns (Sawall et al. 2025), a constant respiration rate over 24 h was assumed for consistency with the traditional approach. Details on the number of replicates used for each treatment and measurement at different sampling times are provided in Table S2.

Variable chlorophyll fluorescence measurements

The measurements of the maximum quantum yield of photosystem II (PSII) of the endosymbionts in the host were conducted on days 0, 7, and 14 using an Imaging Pulse Amplitude Modulated (PAM) Chlorophyll fluorometer (IMAG-MIN/GFP; Heinz Walz GmbH, Effeltrich, Germany), equipped with blue LEDs (470 nm); see details in Ralph et al. (2005). After a 15-min dark acclimation period (Warner et al. 1996; Bhagooli and Hidaka 2004; Gardner et al. 2017; Ben-Zvi et al. 2025), PSII performance was measured for each nubbin on the polyp surface (epithelium) by selecting, via the software (Imaging-WIN v2.32, Heinz Walz GmbH, Effeltrich, Germany), five 'circular' areas of interest (AOI) on the upper part of the polyp. These AOI measurements were averaged to obtain a mean value representative of each nubbin. The maximum quantum yield of PSII was calculated as F_v/F_m (Schreiber 2004), calculated as $F_v/F_m=(F_m\text{-}F_0)/F_m$, where F_m is the maximum fluorescence yield measured during a strong saturation light pulse, and F_0 is the minimum fluorescence yield in the dark acclimated coral sample before the pulse. Settings (Meas. Light Int. 6; Gain 2; Damp 3; Sat. Pulse Int. 8) were adjusted before measurements in the imaging system software, as reported by Schlotheuber et al. (2024).

Microsensors measurements

Electrochemical O_2 microsensors with a tip diameter of 25 µm (OX-25, Unisense A/S, Denmark) were used to measure the O_2 distribution inside the GVC and over the external tissue surface (epithelium, ectoderm) of corals on days 0, 7, and 14 during the heat exposure (Fig. 1). Similarly, electrochemical H_2O_2 microsensors were setup according to Ousley et al. (2022) and used to measure H_2O_2 profiles over the external tissue surface in the same corals. H_2O_2 was not measured in the GVC due to previously known interferences between the hydrogen peroxide microsensor and nitrogen compounds present in this compartment (Ousley et al. 2022). For the external tissue surface measurements, profiles were measured from the surface of the external tissue upward into the surrounding seawater, and the measurement was started after the signal had stabilized.

For microsensor measurements, coral nubbins (n = 3 per condition) were placed inside a custom-built laminar flow chamber connected to a water pump immersed in a reservoir with thermostated and aerated seawater (Fig. S2). See Brodersen et al. (2014) and Haro et al. (2019) for the detailed description of the laminar flow chamber. During the measurements, corals were exposed to the same photon irradiance and temperature conditions as in the experimental aquaria. After being placed in the flow chamber, the corals

were acclimated for 15–20 min before measurements were taken. Additional time was allowed for GVC measurements to ensure full relaxation and mouth opening.

The O_2 microsensor was linearly calibrated from sensor signal readings in 100% air-saturated seawater and anoxic water (using a sodium ascorbate solution) at experimental temperature and salinity. For the H_2O_2 microsensor calibration, 500 mL of seawater from the experimental aquarium was used for 0 concentration measurements, followed by measurements during stepwise addition of 5 µL from a 3% w/v H_2O_2 solution, i.e., a concentration increase of 8.8 µmol L^{-1} at each step. Six steps were conducted, resulting in a final concentration of 52.8 µmol L^{-1}. The microsensors were mounted on a motorized micromanipulator system (Unisense A/S, Denmark) and were connected to a microsensor meter (fx-6 UniAmp, Unisense A/S, Denmark). The micromanipulator and the microsensor meter were connected to a PC with dedicated software for data acquisition and sensor positioning (SensorSuite Profiler v3.2, Unisense A/S, Denmark). The approaching and positioning of the microsensor tip relative to the coral tissue surface and the coral mouth were controlled by the motor in 20-µm steps and visually guided using a digital microscope (Dino-Lite 5MP Edge, AnMo Electronics, Taiwan), to avoid direct contact (see examples in Fig. S3). The measurement profile was conducted with a step size of 100 µm. After each step, the signal was allowed to stabilize for six seconds, followed by a three-second measurement period during which the average signal was recorded. Here, O_2 levels greater than atmospheric saturation (230 µmol O_2 L^{-1}) are referred to as hyperoxic, levels between 180 and 230 µmol O_2 L^{-1} as normoxic, levels between 10 and 180 µmol O_2 L^{-1} as hypoxic, and levels below 10 µmol O_2 L^{-1} as anoxic, in line with Gattuso et al. (2015).

Quantification of chlorophyll a and c2

Quantification of chlorophyll *a* and *c2* was determined in the external tissue surface that was airbrushed from coral samples (Fig. 1), which had been stored at -80 °C since the end of the experiment (Isa et al. 2024). For pigment extraction, ice-cold phosphate-buffered saline (PBS) was first added to tissue samples, and the resulting suspension was mechanically homogenized by repeated passage through a syringe needle and then centrifuged (3600 × g for 4 min). The supernatant was removed, and the remaining pellet was resuspended in 100% acetone and incubated for 24 h in the dark at 4 °C. After extraction, the sample was centrifuged again (3,600 × g for 4 min), and the supernatant was used to determine chlorophyll *a* and *c2* concentrations from absorbance measured in a standard 1 cm wide cuvette on a spectrophotometer (Jasco V-730 UV–Vis, USA) at 630 nm, 663 nm, and 750 nm applying dinoflagellate-specific equations (Jeffrey and Humphrey 1975). Chlorophyll concentrations were normalized to tissue fresh weight (fw).

Analysis of oxidative stress biomarkers in the coral gastrodermis

At the end of the experiment on day 14, each polyp was cut in half with a scalpel, and the gastrodermis was carefully separated from the inner part of each polyp using an airbrush (Fig. 1). The gastrodermis tissue was collected and stored at -80 °C prior to further analysis. Frozen coral gastrodermis samples were crushed with a pre-cooled mortar and pestle, transferred to tubes, and homogenized in lysis buffer (50 mM Tris–HCl, pH 7.4, 150 mM NaCl, 10% glycerol, 1% NP40 detergent, 5 mM EDTA) and a protease inhibitor cocktail and PMSF (phenylmethylsulfonyl fluoride) as previously reported (Montalbetti et al. 2022a, 2022b). After centrifugation (4,400 × g at 4 °C for 10 min) to remove any skeletal debris, the supernatant was divided into aliquots that were used for protein quantification and biomarker analyses, respectively. Aliquots that were not immediately processed were stored at -80 °C until further analyses.

Total protein content was determined using Bradford's colorimetric detection and spectrophotometric quantification method (using a UV–VIS spectrophotometer; Jasco V-730, Jasco Inc., USA) using bovine serum albumin (BSA) for the calibration curve (Bradford 1976). Analyses of the activity of SOD and CAT were performed as previously reported (Isa et al. 2025). Briefly, SOD competes with ferricytochrome *c* to quench O^{2-} radicals; its activity is indicated by its capacity to inhibit the reduction of ferricytochrome *c* by O_2^-, which is generated in the xanthine/xanthine oxidase system. The reaction mixture consisted of ferricytochrome *c* (0.01 mM), EDTA (0.1 mM), xanthine (0.01 mM), and xanthine oxidase (0.0061 U) in a final volume of 1 mL, with all reagents sourced from Sigma-Aldrich. The reduction rate of ferricytochrome *c* was monitored spectrophotometrically at 550 nm. Under these conditions, one unit of SOD activity was defined as the amount of enzyme that achieves 50% inhibition of ferricytochrome *c* reduction. Results are reported as enzyme units (U) per mg of protein.

The activity of CAT was analyzed considering the peroxidative function of the enzyme, based on the method of enzyme degradation of hydrogen peroxide. A reaction solution (containing 50 mM sodium phosphate buffer at pH 7.5 and 12 mM H_2O_2) was added to a 1 mL cuvette with different sample volumes. The decrease in H_2O_2 was followed spectrophotometrically at 240 nm (Varian Cary 50 Scan spectrophotometer, Agilent Technologies). The results are expressed as units (U) of enzyme per mg of protein, where

U refers to k, the first-order kinetic constant (min^{-1}), as previously described (Aebi 1984).

Lipid peroxidation was assessed according to Montalbetti et al. (2021) via malondialdehyde (MDA) quantification using an MDA assay kit (Bioxytech LPO-586, Oxis International, United States). The method is based on the reaction of N-methyl-2-phenylindole with MDA. Gastrodermis samples were pulverized and homogenized in 1 mL of 20 mM phosphate buffer, pH 7.4, with the addition of 0.5 M butylated hydroxytoluene in acetonitrile to prevent oxidation. Following sample centrifugation (3,000 × g at 4 °C for 10 min), the assay (based on the hydrochloric acid solvent method) was performed according to the manufacturer's instructions. The blue product was quantified by measuring absorbance at 586 nm (Gérard-Monnier et al. 1998). Results are presented in µmol MDA $µg^{-1}$ protein.

Statistical analysis

All data were checked for outliers using Iglewicz and Hoaglin's test for multiple outliers (two-sided test, Z score 3,5), normality using the Shapiro–Wilk test, and homoscedasticity of the variance using an F-test. Both normality and variance tests were conducted in R software v 4.3.3 (R Core Team 2024) combined with RStudio v2025.05.0+496 (Posit team 2025). For data that were not normally distributed (even after log transformation, i.e., for pulse amplitude modulated fluorometry, respirometry, and microsensor analysis), a Generalized Linear Mixed Model (GLMM) was used, incorporating fixed effects for Condition, Time, and the interaction term (Time*Condition), as well as random effects to account for repeated measures (Sample ID). Post-hoc pairwise comparisons were performed using Tukey HSD to assess differences between conditions and time points. Pairwise comparisons were performed using the '*emmeans*' package (Lenth et al. 2024). A 2-way ANOVA was employed to test the main effects of Condition, Time, and the interaction term (Time*Condition) in enzyme activities, LPO (after log transformation), and chlorophyll content. The results were visualized with the '*ggplot2*' package (Wickham 2016). All the data related to the models used, such as chi-squared, marginal R^2 (R^2m, marginal coefficient of determination, which represents the variance explained by the fixed factors), and conditional R^2 (R^2c, which represent the variance explained by both fixed and random effects) as previously described by (Bartoń 2020), are available in the Supplementary Material section (Table S3–S6).

Results

Bulk metabolic measurements

No temporal or condition-dependent changes in respiration rate were detected in *C. curvata* (GLMM, all $p>0.05$; Table S3). In contrast, *G. fascicularis* showed a significant effect of condition in the overall model ($\chi^2=77.6$, $p<0.05$, $R^2m=0.05$; Table S3), with higher respiration rates under heat stress (controls 0.77 ± 0.28 µmol O_2 cm^{-2} h^1 mean ± SD, heat stress 1.21 ± 0.65 µmol O_2 cm^{-2} h^{-1}, Fig. 2a). However, no significant differences among conditions for each sampling day for *G. fascicularis* were observed.

Net photosynthesis (P_{net}) in *C. curvata* showed differences over time (GLMM, $\chi^2=78.8$, $p<0.01$), and in the interaction between time and conditions ($\chi^2=84.5$, $p<0.05$, $R^2m=0.33$; Fig. 2b, Table S3). Controls exhibited higher P_{net} on day 0 compared to heat-stressed corals (1.22 ± 0.73 vs. 0.24 ± 0.58 µmol O_2 cm^{-2} h^{-1}; $p<0.001$; Table S4),

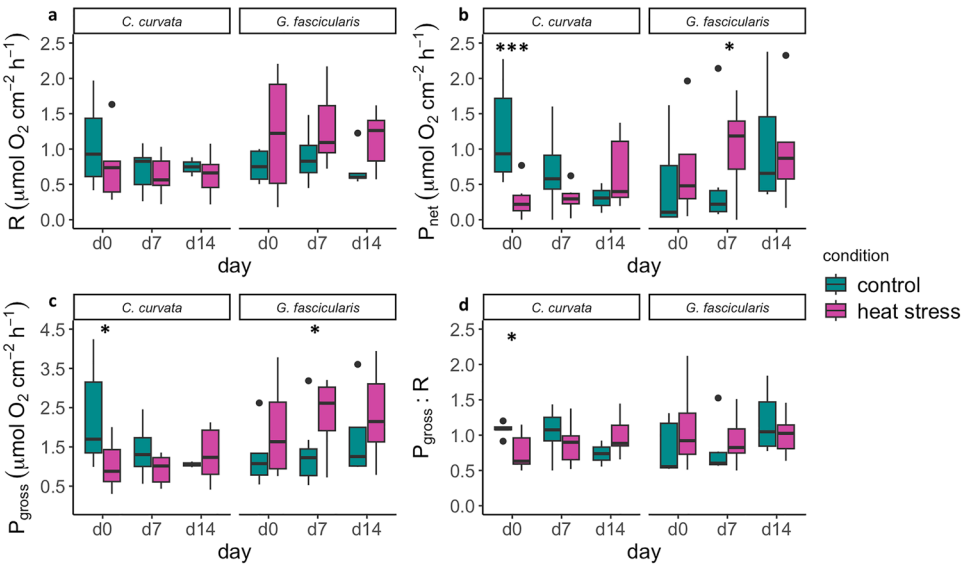

Fig. 2 Bulk metabolic measurements on colonies of *C. curvata* (n = 4 per tank per condition per day) and *G. fascicularis* (n = 4 per tank per condition per day) quantifying dark respiration, R (**a**), net photosynthesis, P_{net} (**b**), gross photosynthesis, P_{gross} (**c**), and the ratio of gross photosynthesis to respiration, P_{gross}:R (**d**). Measurements were recorded on days 0, 7, and 14 of exposure to control (green) and heat stress (purple) conditions. Boxplots represent the median, interquartile range, and extreme values for each condition and time point. Asterisks denote treatment is significantly different from the control on each day (* $p<0.05$; *** $p<0.001$; Tukey HSD for pairwise comparison tests, Table S4)

suggesting a recovery or stabilization over time for this species. For *G. fascicularis,* a significant increase in P_{net} under heat stress on day 7 was detected (controls: 0.47 ± 0.44 vs heat stress: 1.04 ± 0.65 µmol O_2 cm^{-2} h^{-1}; $p < 0.05$; Table S4), in which a transient photosynthetic enhancement occurs during the exposure period.

No detectable effect of heat stress on P_{gross} for either species was detected by the overall model ($R^2m = 0.21$ for *C. curvata*, $R^2m = 0.15$ for *G. fascicularis*; Fig. 2c, Table S3). However, *C. curvata* controls had higher values on day 0 (2.28 ± 1.35 µmol O_2 cm^{-2} h^{-1}; $p < 0.05$), while *G. fascicularis* heat-stressed nubbins recorded higher values on day 7 (2.33 ± 0.95 µmol O_2 cm^{-2} h^{-1}; $p < 0.05$; Tab. S4).

Effects of heat stress on the P_{gross}:R ratio were recorded in the overall model across time per condition (GLMM, $\chi^2 = 79.1$, $p < 0.05$, $R^2m = 0.19$) for *C. curvata*, with significant differences among conditions at day 0 (controls: 1.08 ± 0.09 vs heat stress: 0.77 ± 0.30; $p < 0.05$; Table S4). The overall model indicated differences among conditions for *G. fascicularis* ($\chi^2 = 67.1$, $p < 0.05$, $R^2m = 0.17$; Fig. 2d, Table S3).

On day 14, no differences were found for either species or any of the metabolic rate parameters. These results suggest transient, species-specific responses to heat stress.

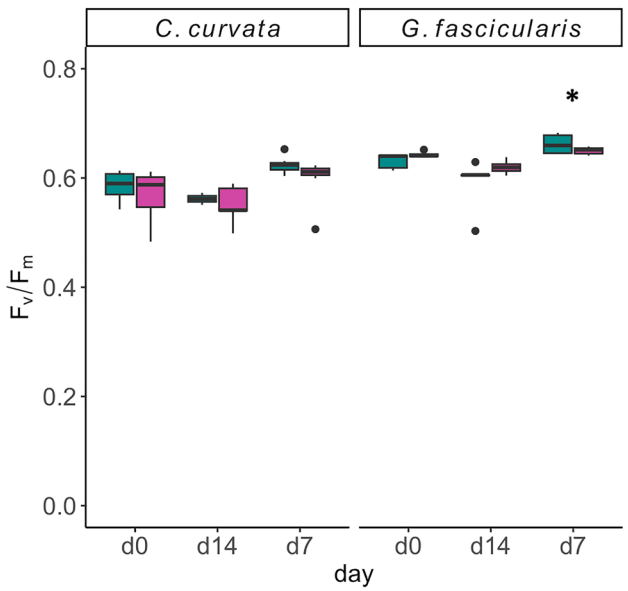

Fig. 3 Maximum PSII quantum yield (F_v/F_m) of symbionts *in-hospite* measured in control and heat-stressed coral conditions over time. F_v/F_m values (mean ± SD, n = 7) for the two coral species (*C. curvata* and *G. fascicularis*) on days 0, 7, and 14 of exposure to control (green) and heat stress (purple) conditions. Boxplots represent the median, interquartile range, and extreme values for each condition and time point. Asterisks denote treatment is significantly different from the control on each day (* $p < 0.05$; Tukey HSD for pairwise comparison tests, Table S4)

Variable chlorophyll fluorescence measurements

Both *C. curvata* and *G. fascicularis* showed lower maximum PSII quantum yield (F_v/F_m) in the heat stress conditions according to the overall model (GLMM, $\chi^2 = 116.6$, $p < 0.01$, $R^2m = 0.32$ for *C. curvata*; $\chi^2 = 301.9$, $p < 0.001$, $R^2m = 0.51$ for *G. fascicularis*, Table S3). Mean values decreased slightly over time in nubbins subjected to heat stress (for *C. curvata,* 0.57 ± 0.04 vs controls: 0.59 ± 0.02; mean ± SD; for *G. fascicularis,* 0.64 ± 0.01 vs. controls: 0.63 ± 0.03). Nevertheless, no differences were observed at individual times, except on day 14 for *G. fascicularis* ($p < 0.05$; Fig. 3, Table S3), with higher values (~7%) recorded in heat-stressed nubbins. Across the experiment, F_v/F_m values remained relatively high in both species; for *C. curvata,* mostly above 0.55, and for *G. fascicularis*, above 0.60. By day 14, control corals generally maintained values above 0.55, while heat-stressed corals displayed greater variability. For both conditions on day 14, some values dropped close to 0.50.

Microsensors measurements of O_2

The O_2 levels within the GVC of *C. curvata* and *G. fascicularis* were significantly affected by heat stress. The overall model for *C. curvata* recorded differences across time (GLMM, $\chi^2 = 2{,}118{,}716$, $p < 0.001$), conditions ($\chi^2 = 68{,}588$, $p < 0.01$, $R^2m = 0.42$), and for the combination of time per conditions ($\chi^2 = 1{,}655{,}493$, $p < 0.001$; Fig. 4, Table S5), with lower O_2 values in heat-stressed corals (201 ± 138 µmol O_2 L^{-1}, mean ± SD) compared to the controls (344 ± 94 µmol O_2 L^{-1}). In *G. fascicularis,* differences in the O_2 within the GVC by the model across time ($\chi^2 = 2{,}149{,}631$, $p < 0.001$, $R^2m = 0.40$) and for the combination time per conditions ($\chi^2 = 434{,}176$, $p < 0.001$; Fig. 4, Table S5), with lower concentration under heat stress conditions (238 ± 136 µmol O_2 L^{-1} compared to 272 ± 66 µmol O_2 L^{-1} in the controls).

On day 0, hyperoxic conditions in control coral nubbins were recorded in both coral species, with values ≥ 600 µmol O_2 L^{-1} for *C. curvata* and > 450 µmol O_2 L^{-1} for *G. fascicularis*. By the end of the exposure, heat-stressed corals exhibited a marked decline in O_2 levels in the GVC. This resulted in anoxic conditions (0 µmol O_2 L^{-1}) in two *C. curvata* nubbins and hypoxic conditions (< 100 µmol O_2 L^{-1}) for *G. fascicularis* ones. Compared to controls, which maintained levels exceeding 200 µmol O_2 L^{-1}, a ~ 90% decrease was recorded in heat-stressed corals, reaching strongly hypoxic conditions (approximately 20 µmol O_2 L^{-1} for *C. curvata* and 90 µmol O_2 L^{-1} for *G. fascicularis,* on average). This difference was statistically significant for both species (*C. curvata*: $p < 0.001$; *G. fascicularis*: $p < 0.01$; Fig. 4, Table S5).

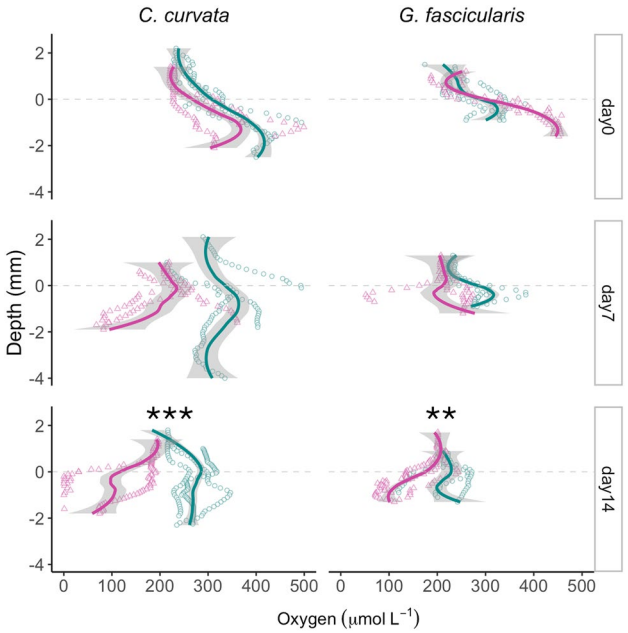

Fig. 4 Concentration profiles of O_2 measured in the gastrovascular cavity (CVC) of *C. curvata* and *G. fascicularis* after 0, 7, and 14 days of exposure to control (green) and heat stress (purple) conditions under a downwelling photon irradiance (400–700 nm) of 150 µmol photons m^{-2} $s.^{-1}$. The zero depth and grey dashed line indicate the level of the coral mouth opening, while negative and positive depths indicate positions above and inside the GVC, respectively. Continuous lines indicate the trend line of the means of the three profile values, while shaded grey areas indicate 95% confidence intervals. Oxygen values in individual profiles (1 profile per nubbin, n = 3 nubbins per condition per time) are shown with symbols (circles for control and triangles for heat stress, in the color of the condition). Asterisks denote cases where the O_2 profile in heat-treated corals differed significantly from the control on each day (** $p < 0.01$; *** $p < 0.001$; Tukey HSD for pairwise comparison tests, Table S6)

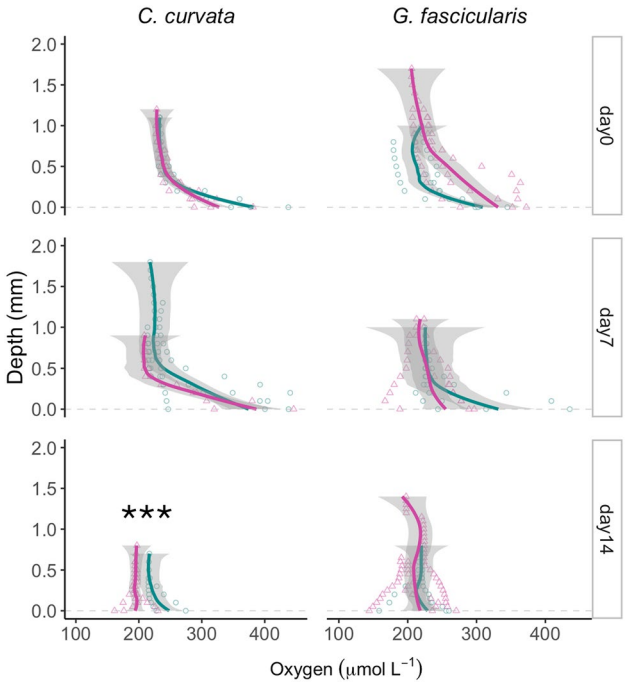

Fig. 5 Concentration profiles of O_2 measured towards the external tissue surface of *C. curvata* and *G. fascicularis* after 0, 7, and 14 days of exposure to control (green) and heat stress (purple) conditions under a downwelling photon irradiance (400–700 nm) of 150 µmol photons m^{-2} $s.^{-1}$. Zero depth and the grey dashed line indicate the coral external tissue surface. Continuous lines indicate the trend line of the means of the three profile values, while the shaded grey areas indicate 95% confidence intervals. Oxygen values in individual profiles (1 profile per nubbin, n = 3 nubbins per condition per time) are shown with symbols (circles for control and triangles for heat stress, in the color of the condition). Asterisks denote cases where the O_2 profile in heat-treated corals differed significantly from the control on each day (*** $p < 0.001$; Tukey HSD for pairwise comparison tests, Table S6)

Measurements of O_2 concentration over the coral external tissue surface revealed similar overall trends to those observed in the GVC profiles, where O_2 availability at the external tissue surface of both species was impaired in the heat stress condition. For *C. curvata,* differences across time ($\chi^2 = 997{,}631$, $p < 0.001$, $R^2m = 0.36$) and conditions (controls 259 ± 67 µmol O_2 L^{-1} vs heat stress 232 ± 49 µmol O_2 L^{-1}; $\chi^2 = 86{,}038$, $p < 0.01$; Fig. 5, Table S5) were recorded in the overall model. For *G. fascicularis,* differences in O_2 levels were found across time ($\chi^2 = 423{,}862$, $p < 0.001$, $R^2m = 0.20$) and for the interaction of time and conditions (controls: 232 ± 43 µmol O_2 L^{-1} vs heat stress: 229 ± 42 µmol O_2 L^{-1}; $\chi^2 = 426{,}277$, $p < 0.001$; Fig. 5, Table S5). Hyperoxic conditions were recorded on days 0 and 7 at the external tissue surface, with values exceeding 400 µmol O_2 L^{-1} for both species. By day 14, a significant decrease in O_2 concentration (~29%) was measured at the external tissue surface of *C. curvata* ($p < 0.001$; Fig. 5, Table S6), with heat-stressed nubbins showing a mean reduction of 30 µmol O_2 L^{-1}.

Microsensors measurements of H_2O_2

At the coral external tissue surface, H_2O_2 concentration showed variation patterns in the two species. Differences across conditions were revealed by the overall model in *C. curvata* ($\chi^2 = 0.9$, $p < 0.01$, $R^2m = 0.04$), with lower H_2O_2 levels under heat stress (controls: 0.17 ± 0.24 µmol H_2O_2 L^{-1} vs heat stress: 0.12 ± 0.20 µmol H_2O_2 L^{-1}; mean ± SD), while for *G. fascicularis,* differences were observed for the combination of time per conditions ($\chi^2 = 239{,}794$, $p < 0.001$), with lower values under heat stress (controls: 0.24 ± 0.53 µmol H_2O_2 L^{-1} vs heat stress: 0.16 ± 0.37 µmol H_2O_2 L^{-1}; Fig. 6, Table S5). A significant H_2O_2 concentration decrease under heat stress conditions, as compared to the control, was recorded at day 0 for *G. fascicularis* ($p < 0.01$, Table S6). It is important to highlight that at day 0, both groups were kept at the same temperature (25 °C) and were not yet subjected to the heat stress treatment. While the H_2O_2 concentration in *C. curvata* rarely exceeded 1 µmol H_2O_2 L^{-1}, 13 measurements showed higher values at the coral external tissue

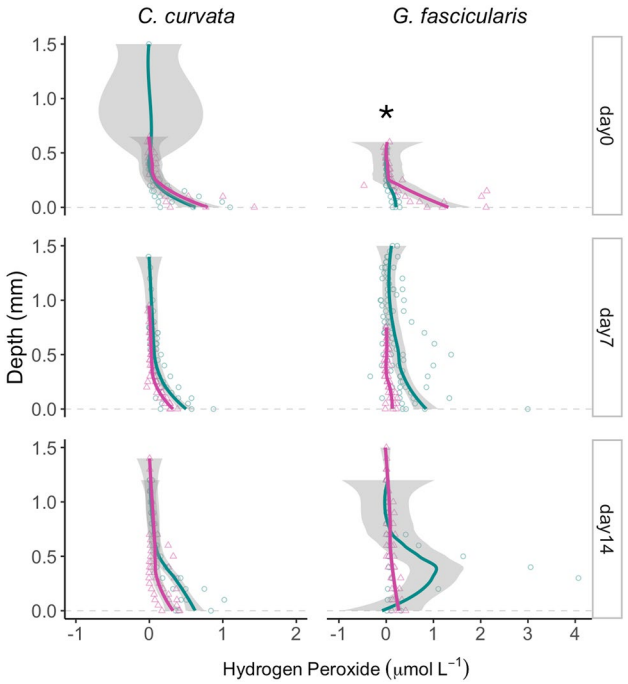

Fig. 6 Hydrogen peroxide (H_2O_2) concentration profiles measured towards the external tissue surface of *C. curvata* and *G. fascicularis* after 0, 7, and 14 days of exposure to control (green) and heat stress (purple) conditions under a downwelling photon irradiance (400–700 nm) of 150 µmol photons m^{-2} $s.^{-1}$. Zero depth and the grey dashed line indicate the polyp surface level. Continuous lines indicate the trend line of the means of the three profile values, while the shaded grey areas indicate 95% confidence intervals. Hydrogen peroxide values in individual profiles (1 profile per nubbin, n = 3 nubbins per condition per time) are shown with symbols (circles for control and triangles for heat stress, in the color of the condition). Asterisks denote cases where the H_2O_2 profile in heat-treated corals differed significantly from the control on each day (* $p < 0.05$; Tukey HSD for pairwise comparison tests, Table S6)

surface of *G. fascicularis*. The highest H_2O_2 concentrations were recorded at 0.3 mm (4.1 µmol H_2O_2 L^{-1}) and 0.4 mm (3.1 µmol H_2O_2 L^{-1}) above the external tissue surface on day 14 under control conditions.

Quantification of chlorophyll *a* and *c2*

After 14 days of heat stress exposure, no significant changes in Chl *a* or *c2* concentration were observed between heat-stressed corals and control conditions for both coral species. However, chlorophyll concentration differed significantly among the two species, with lower values in *G. fascicularis* (< 10 µg Chl g^{-1} fw) compared to *C. curvata* (~ 35 µg Chl g^{-1} fw) under both control and heat-stress conditions (Fig. 7, Table 1).

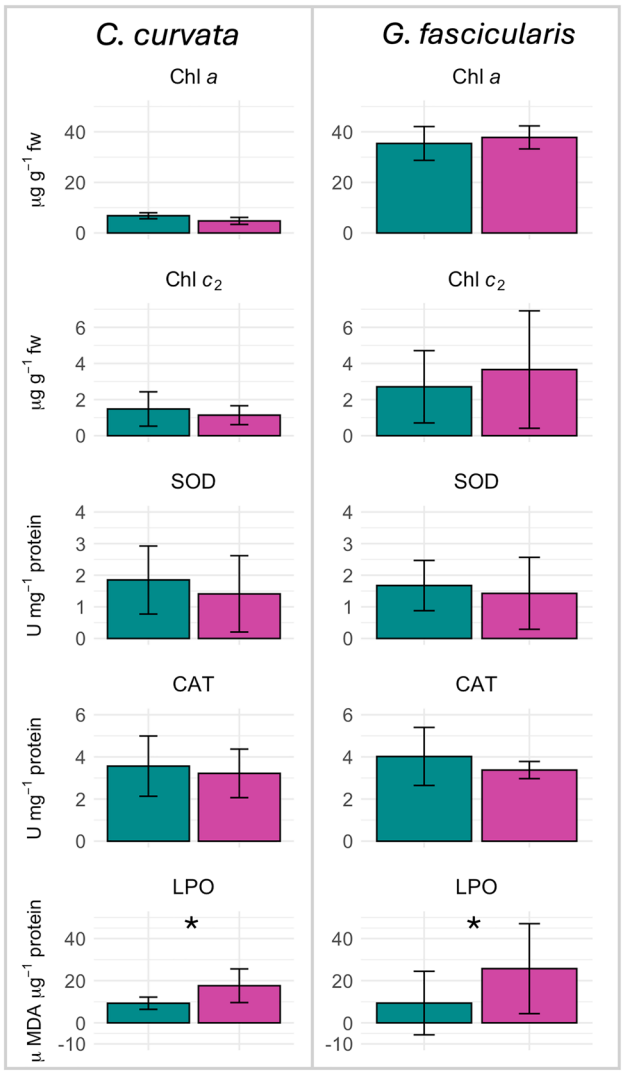

Fig. 7 Chlorophyll (Chl) concentration and oxidative stress biomarkers in the gastrodermis. The concentration of Chl *a* and Chl *c2*, and the activity of superoxide dismutase (SOD), catalase (CAT), and lipid peroxidation (LPO) were measured in *C. curvata* (left panels) and *G. fascicularis* (right panels) in control (green) and 14-day heat-stressed (purple) samples of the two coral species. Chlorophyll concentrations were normalized to tissue fresh weight (g fw). Enzyme activity of SOD and CAT is expressed in units (U) of enzyme per mg protein in the coral, while LPO activity is expressed as µM malondialdehyde (MDA) per µg protein. The data are presented as mean ± SD (n = 4 per treatment), and asterisks denote a significantly different effect of the temperature treatment (2-way ANOVA, Table S7)

Analysis of oxidative stress biomarkers in the gastrodermis

In the heat-stressed corals, no significant changes in the SOD and CAT activity in the gastrodermis were recorded between species, within each species, or between conditions (Fig. 7, Table S7). However, MDA levels, indicative of LPO, were higher in the gastrodermis of heat-stressed coral specimens for both coral species (two-way ANOVA, $p < 0.05$,

Table 1 Summary of results obtained for all the parameters analyzed in the two coral species subjected to heat stress at different exposure days

Parameters:		Heat Stress Day 0	Heat Stress Day 7	Heat Stress Day 14
Caulastrea curvata				
Bulk metabolic measurements	R	=	=	=
	P_{net}	↓	=	=
	P_{gross}	↓	=	=
	P_{gross}:R	↓	=	=
Variable chlorophyll fluorescence	F_v/F_m	=	=	=
Microsensor measurements	O_2 in the GVC	=	=	↓
	O_2 external tissue surface	=	=	↓
	H_2O_2 external tissue surface	=	=	=
Chlorophyll concentrations	Chl *a*	–	–	=
	Chl *c2*	–	–	=
Biochemical analyses of the gastrodermis	SOD	–	–	=
	CAT	–	–	=
	LPO	–	–	↑
Galaxea fascicularis				
Bulk metabolic measurements	R	=	=	=
	P_{net}	=	↑	=
	P_{gross}	=	↑	=
	P_{gross}:R	=	=	=
Variable chlorophyll fluorescence	F_v/F_m	=	=	↑
Microsensor measurements	O_2 in the GVC	=	=	↓
	O_2 external tissue surface	=	=	=
	H_2O_2 external tissue surface	=	=	↑
Chlorophyll concentrations	Chl *a*	–	–	=
	Chl *c2*	–	–	=
Biochemical analyses of the gastrodermis	SOD	–	–	=
	CAT	–	–	=
	LPO	–	–	↑

The '↑' symbol indicates a significant increase in the parameter, while the '↓' symbol indicates a significant decrease (based on Tukey HSD for pairwise comparison tests). Non-significant deviations are indicated by '=', while the '/' symbol indicates that the measurement was not carried out on that day

Table S7). In *C. curvata*, MDA levels in the gastrodermis of heat-stressed nubbins increased by about 90%, while in *G. fascicularis*, these levels increased by about 198%, as compared to corals under control conditions (Fig. 7).

A schematic summary of the results is provided in Table 1.

Discussion

Thermal stress can trigger highly localized changes within internal compartments of corals in terms of oxygen dynamics and prelethal oxidative stress, which may not be evident in larger-scale, integrative measurements. Overall, we demonstrated that heat stress drives oxygen depletion in the GVC and alters prelethal oxidative stress dynamics, despite a relatively stable respiration, photosynthesis, and chlorophyll content measured at the holobiont level (Table 1). These findings underscore the need to investigate compartment-specific dynamics, as bulk physiological measurements alone may not capture subtle, yet functionally significant changes occurring at the microscale (Bollati et al. 2024).

Bulk metabolic measurements of respiration and photosynthesis

After 14 days, respiration rates remained comparable between the control and heat-stressed corals in both species. Total respiration measured at the level of the coral holobiont reflected the combined activity of the host, symbiotic algae, and associated microbes (Muscatine et al. 1981; Haas et al. 2011). Since overall respiration rates did not change under thermal stress, the relative contributions of these components may have remained stable. Alternatively, thermal stress may have induced opposing shifts in the metabolic activity of the components, such as increased respiration in some and decreased activity in others, resulting in a final balance at the holobiont level. By the end of the exposure period, there were no significant differences in $P_{gross,}$ P_{net}, or the P_{gross}:R ratio between control and heat stress conditions. Similar stability has been reported in other heat-stressed

tropical coral species, including *G. fascicularis* (Hoadley et al. 2015; Doering et al. 2023).

The bulk metabolic measurements did not show any significant differences in any of the parameters analyzed at the end of the heat exposure. This might be attributed to a certain degree of thermal resistance in the two species studied, albeit the mechanisms for such resistance are hard to identify from such holobiont-level measurements. The ecophysiology of corals, as well as their adaptive capacity, can be influenced by association with different taxa of zooxanthellae (Bhagooli and Hidaka 2003; Ulstrup et al. 2006; Cooper et al. 2011; Torres et al. 2021; Parkinson et al. 2025). The relative thermal resilience observed in our results might be at least partially affected by a shift of symbionts toward more temperature-tolerant clades, as *G. fascicularis* can host the dinoflagellate genera *Cladocopium* (formerly clade C) and *Durusdinium* (formerly clade D) (Puntin et al. 2023). Under typical environmental conditions, *Cladocopium* is the primary symbiont. However, a shift in symbiont dominance from *Cladocopium* to *Durusdinium*, which is known for its higher thermal tolerance (Matsuda et al. 2022), has been previously observed (Puntin et al. 2023). For the genus *Caulastrea*, the most prevalent symbiont type is *Cladocopium* (Raijmakers 2024). Coral's harboring *Durusdinium* are more thermotolerant than those harboring *Cladocopium* (Wang et al. 2023). Therefore, we speculated that shifts in symbiont dominance may have contributed to the observed resilience.

Variable chlorophyll fluorescence measurements

Variable chlorophyll fluorescence measurements (pulse-amplitude-modulation fluorometry—PSII performance) showed an increase in the maximum PSII quantum yield (F_v/F_m) from day 0 to day 7, followed by a decrease on day 14. F_v/F_m values above 0.60 are generally associated with healthy corals, while values below 0.50 typically indicate ongoing stress and impaired PSII performance of the symbionts (Schoepf et al. 2018). The low F_v/F_m values observed for *C. curvata* on day 0 may suggest an incomplete acclimatization period, as some nubbins exhibited relatively low values despite the pre-experimental stabilization phase. Similarly, *G. fascicularis* showed an increase in F_v/F_m values from day 0 to day 7, although the initial values were higher than those of *C. curvata*. This could suggest that incomplete acclimation may have affected this species as well. Although a stabilization period of 7–12 days is generally considered sufficient for experimental acclimatization in corals (Grottoli et al. 2021), this species may require a longer acclimation period. Nevertheless, by day 7, F_v/F_m increased to values above 0.60 for both treatments and species, suggesting a return to a healthy physiological state. Cheng et al. (2024) found that F_v/F_m values in *G. fascicularis* were not significantly affected by heat stress after 96 h exposure at + 3 °C (control at 29 °C). Similarly, a significant decrease in F_v/F_m over time in the high-temperature treatment in *G. fascicularis*, with reduced yields also observed in the control corals, was reported in a previous study (Doering et al. 2023). These findings were consistent with our results, which showed a slight decrease in mean F_v/F_m values under heat stress and relatively high values that are maintained throughout the experiment under both conditions. Although a decrease in F_v/F_m was observed on day 14 in both experimental conditions compared to day 7 (with no difference between conditions), bulk metabolic measurements of photosynthesis did not show a decrease over time (indeed, net and gross photosynthesis appeared to have higher values over time). This suggests that the decrease in F_v/F_m may not be indicative of a true decrease in net or gross photosynthesis. Possibly, the decrease in F_v/F_m reflected increased physiological stress at the photosystem level without immediately compromising overall photosynthetic capacity. Shallow-water corals show seasonal and diurnal variations in quantum yield, with the lowest values during the late summer months (Warner et al. 2002). The reversible down-regulation of zooxanthellae's photosynthetic activity (Long et al. 1994) involves the dissipation of excess energy through a photoprotective process to avoid damage to PSII by dissipating heat within reaction centers (Niyogi 1999; Gorbunov et al. 2001). A photoprotective process known as non-photochemical quenching (NPQ) of chlorophyll fluorescence prevents photodamage under stress (Brown et al. 1999; Warner and Berry-Lowe 2006; Derks et al. 2015; Buck et al. 2019). When NPQ increases, a reduction in F_v/F_m values is recorded, with decreased efficiency (Berteotti 2015). Under elevated temperatures, NPQ is an important photoprotective mechanism in the coral zooxanthellae that helps to dissipate excess energy (Hill et al. 2004, 2005; Middlebrook et al. 2008; Hennige et al. 2009). The observed reduction in PSII performance, which occurred in both conditions, could also be due to photoacclimatization rather than photoinhibition, as already found in previous studies (Robison and Warner 2006; Hennige et al. 2009; Krämer et al. 2012).

Microenvironment of the coral gastrovascular cavity

Oxygen levels in the upper GVC, as well as in the tissue layer surface and the associated diffusive boundary layer (DBL), are highly variable as they are influenced by daily light cycles and resulting variations in coral tissue oxygenation (Shashar et al. 1996). The surface of the external tissue, which is lined by ciliated cells, contributes to this variability by modifying the local mass transfer with the surrounding water (Hughes et al. 2022; Pacherres et al.

2022). In contrast, deeper parts of the GVC can exhibit low O_2 conditions or anoxia even under continuous light (Agostini et al 2012; Bove et al. 2020). The O_2 dynamic in the coral GVC is highly variable across species (Bollati et al. 2024) and can be strongly influenced by the coral structure and tissue plasticity (e.g., Dellisanti et al. 2024).

In our study, corals subjected to thermal stress showed significant decreases in the GVC O_2 concentration reaching hypoxic/anoxic conditions after 14 days of exposure, as compared to the controls that remained normoxic or hyperoxic. The reduction of O_2 in the GVC can be explained as the increase in respiration by the holobiont, as already suggested by Agostini et al. (2012). However, this hypothesis is not supported by our bulk metabolic measurements showing no significant differences between conditions for either species. Hypoxic conditions could also be triggered by the high metabolic activity of bacteria living in the microenvironment of the GVC of the coral polyp, which is known to harbor a distinct microbiome (Bollati et al. 2024). According to Riedel et al. (2013), nutrient availability plays a critical role in influencing respiration rates in bacteria. The richness of nutrients in the GVC compared to the surrounding water (Agostini et al. 2012), combined with elevated temperatures, may further stimulate bacterial metabolism (Manning et al. 2018). Lowest O_2 levels were recorded in the deeper regions of the GVC, where hypothetically and according to our results, interactions with the water surrounding the holobiont is minimal. Therefore, the observed O_2 decline in the GVC might be explained by the metabolic activity of its associated bacterial community. Bollati et al. (2024) found that the coral GVC microbiome was mainly composed of microaerophilic or facultatively anaerobic microbial communities such as *Epsilonproteobacteria* (formerly *Campylobacterota*), a class of Proteobacteria already known as gut symbionts of other marine invertebrates (Hakim et al. 2015).

The decrease in O_2 levels in the coral GVC with increasing temperatures could also be attributed to reduced availability or reduced uptake rates of organic and inorganic nutrients required for photosynthesis by symbiotic algae (Yellowlees et al. 2008; Rädecker et al. 2015; Tansik et al. 2017). High temperatures can limit the coral uptake rate of some nutrients, such as nitrate and ammonium. Disruption of the homeostatic balance of inorganic nutrients during thermal stress plays a role in host immunity and dysregulation of the coral symbiosis (Weis 2019). These limitations may also have occurred within the GVC, which would have led to reduced photosynthesis and reduced oxygen production.

On the other hand, *G. fascicularis* nubbins under control conditions showed normoxia/hyperoxia in the GVC under an incident photon irradiance (400–700 nm) of 150 µmol photons m^{-2} s^{-1}, while Agostini et al. (2012) and Bollati et al. (2024) reported hypoxic/anoxic conditions, even under prolonged illumination, for the same species under 200 µmol photons m^{-2} s^{-1} and 650 µmol photons m^{-2} s^{-1}, respectively. Similarly to our results, normoxic or hyperoxic conditions were recorded under the light in the GVC of tropical (Bove et al. 2020) and temperate (Dellisanti et al. 2024) corals due to the photosynthetic activity of symbionts. Normoxic or slightly hyperoxic values were recorded by Agostini et al. (2012, 2013) in the upper GVC of *G. fascicularis* in light-exposed specimens. Bollati et al. (2024) suggested that, besides the effects of diffusional exchange between the GVC and the surrounding tissue, microenvironmental changes in the upper GVC may also result from polyp expansion/contraction movements, which increase contact between the upper GVC and oxygenated seawater, creating a ventilation effect. This aeration might be more effective in corals with larger polyps, such as the two species studied in this work the observed oxygen distribution dynamic. Our results indicate that the GVC is a dynamic environment that plays an active role in coral holobiont function and stress resilience.

Coral external tissue surface microenvironment

The external tissue surface O_2 concentrations of control samples in both species were generally above 230 µmol O_2 L^{-1} due to photosynthesis by symbiotic algae in the underlying coral tissue. The hyperoxic and normoxic conditions measured in the DBL by microsensors under light are consistent with data previously recorded for other tropical coral species, including *G. fascicularis* (Agostini et al. 2013; Linsmayer et al. 2020, 2024; Schlotheuber et al. 2024). In our experiment, the tissue surface O_2 concentration was influenced by time and conditions for both species. After 14 days, the O_2 concentration was significantly reduced for the heat-stressed *C. curvata*. Agostini et al. (2013) found differences in the microenvironment near the external tissue surface of heat-stressed corals, with differences in photosynthesis and respiration rates recorded with microsensors. Linsmayer et al. (2024) found a decrease in O_2 at the coral surface as bleaching progressed. In partially bleached colonies, tissue surface O_2 levels were indistinguishable from water column O_2 concentrations and reached lower levels in fully bleached colonies, indicating a loss of O_2 production from photosynthesis due to the ongoing stress (Linsmayer et al. 2024). In contrast, our results showed a local decrease in tissue surface O_2 concentration in the absence of bleaching, indicating a local heat-induced increase in respiration in the coral external tissue surface and/or the immediate mucus layer above. The nature of bleaching cascades, in which single triggers can activate multiple pathways, and multiple stressors can converge toward common endpoints, is complex, and uncertainties persist (Helgoe et al. 2024).

In particular, their analysis highlights how the activation of specific pathways and the resulting outcomes are highly dependent on environmental and biological context, underscoring the need for further research.

Hydrogen peroxide (H_2O_2) dynamics at the coral surface were variable, with no changes under stress. Our findings showed that, while only a few H_2O_2 concentrations exceeded 1 µmol H_2O_2 L^{-1} in *C. curvata*, *G. fascicularis* had 13 cases above this threshold, with peaks of 4.1 µmol H_2O_2 L^{-1} (at 0.30 mm distant from the external tissue surface) and 3.1 µmol H_2O_2 L^{-1} (0.40 mm distant) on day 14 under control conditions. These values and the profiles recorded in this study were consistent with those previously found by Ousley et al. (2022) in *Stylophora pistillata* (Esper, 1792) and *Pocillopora damicornis* (Linnaeus, 1758), and by Schlotheuber et al. (2024) in *P. damicornis*. Similar to a previous study (Schlotheuber et al. 2024), our results showed no evidence of a relationship between heat stress and increased H_2O_2 concentrations at the external coral tissue surface. Moderate heat may accelerate H_2O_2 production in the chloroplasts of algal symbionts by damaging the thylakoid membrane, allowing diffusion to the host cell (Baird et al. 2009), and leading to the expulsion of the symbionts (Dunn et al. 2007). However, some of the measured oscillations in the H_2O_2 levels might also have been affected by interferences, as discussed by Ousley et al. (2022) and by Schlotheuber et al. (2024). According to Ousley et al. (2022), rapid H_2O_2 dynamics showed a rapid signal increase within milliseconds that dissipated over 1–5 s, might be due to mechanical interference, whereas as H_2O_2 concentration bursts from the coral external tissue surface showed a slower dynamic. Increasing H_2O_2 concentration over some minutes were recorded by Armoza-Zvuloni et al. (2016) in *S. pistillata* after feeding and chemical stimuli. In our measurements, we mostly observed burst-like dynamics in H_2O_2 concentrations, indicative of biological production of H_2O_2 rather than interference (Fig. S4b). The latter was, however, also observed with the microsensor tip positioned close to the external tissue surface (Fig. S4a), which may explain our measurements of the highest H_2O_2 concentrations just above this microenvironment. Such H_2O_2 bursts are commonly observed in healthy corals (Ousley et al. 2022; Schlotheuber et al. 2024). Given that the overall H_2O_2 concentrations did not indicate an increase in its production in the external tissue microenvironment under thermal stress, we proposed that such H_2O_2 levels were likely within the coral's ability to maintain H_2O_2 homeostasis.

Chlorophyll concentration and prelethal oxidative stress biomarkers in the gastrodermis

Despite the absence of significant changes in chlorophyll content, SOD and CAT activity, we observed an increase in lipid peroxidation (LPO) in the gastrodermis lining the GVC of heat-stressed corals. Noteworthy, this is the first time that antioxidant enzymes have been analyzed in the gastrodermis of corals. Previous studies on *G. fascicularis* have also reported limited or no modulation of antioxidant enzymes in response to heat stress: Higuchi et al. (2008) found no differences in SOD activity and an increase in CAT levels, while Doering et al. (2023) reported no effect on either enzyme. However, Dias et al. (2019b) found no evidence of oxidative damage in *G. fascicularis*. This species typically hosts thermo-tolerant *Durusdinium* symbionts, and it was identified as the most resistant species to heat stress in the aforementioned study. Our results are consistent with these observations, as neither species we studied showed increased SOD or CAT activity under heat stress conditions. Doering et al. (2023) suggested that such absence of enhanced ROS-related enzyme activity in heat-stressed corals could result from a fast antioxidant response to ROS. Enzymes such as SOD and CAT are typically involved in the early stages of oxidative stress defense, which may become compromised by ROS activity over longer periods of stress. We speculate that corals in our study may have reached a threshold where their antioxidant defense mechanisms were overwhelmed by ROS generated during thermal stress. In this scenario, our finding of enhanced LPO in heat-stressed polyps could indicate that antioxidant defenses were insufficient to counteract ROS accumulation in the gastrodermis, leading to oxidative damage. This pattern aligns with previous studies that detected oxidative damage at the level of whole coral holobionts (Downs et al. 2002; Montalbetti et al. 2021). For instance, Downs et al. (2002) and Montalbetti et al. (2021) demonstrated that while SOD and CAT levels might not always rise during bleaching events, LPO levels increased significantly. This could imply that the corals had reached a point at which their enzymatic defenses were no longer sufficient to counteract the stressors. This suggests that focusing only on antioxidant enzymes might not fully capture the complexity of coral oxidative stress, as ROS can originate from multiple sources, including algal photosynthesis, associated microbiome organisms, or the host coral itself (Hansel and Diaz 2021). Our focus on gastrodermal enzyme activity may have overlooked other sites of ROS generation, such as intracellular production resulting from disrupted photosynthesis in Symbiodiniaceae, mitochondrial electron transport in the coral host (Lesser 2006; Diaz et al. 2016), and extracellular ROS production at the coral surface mediated by host oxidoreductases or

mucus-associated microbes (Saragosti et al. 2010; Diaz et al. 2016). Furthermore, according to Diaz et al. (2016) and Grabb et al. (2019), extracellular superoxide concentrations are dependent on bacterial community composition and coral species. Therefore, coral-associated microbial communities and how they interact with the host during thermal stress need to be better understood.

Low O_2 concentration detected in the GVC reaching hypoxic or anoxic conditions in our heat-stressed corals could have further contributed to the damage of biological membranes, as indicated by the elevated levels of MDA in the polyps' gastrodermis. Indeed, hypoxia can induce the production of intracellular ROS in aquatic invertebrates (Wang et al. 2022; Lee et al. 2022, 2023), and an increase in MDA in response to hypoxia has been reported in *Mytilus galloprovincialis* (Lamarck, 1819), according to the results of Wang et al. (2022). Higher levels of LPO indicate excess ROS that are not neutralized by antioxidants, which can lead to oxidative damage. However, to date, there is no evidence in the coral literature for increased LPO values under low O_2 conditions, and the only other study of anoxia and LPO in corals indicated no changes (Deleja et al. 2022) after overnight exposure to anoxia.

The so-called 'hypoxia paradox' describes the production of ROS under low-oxygen conditions, although these molecules require O_2 for their formation. This phenomenon is related to a malfunction of the mitochondrial respiratory chain, where the blockage of electron flow at the level of complex III (ubiquinone cytochrome *c* reductase) leads to the accumulation of reduced intermediates such as ubisemiquinone (Chandel et al. 1998) that react with the remaining available O_2 to form O_2^- by electron leakage. Additionally, Guzy and Schumacker's (2006) suggested that the respiratory electron transport chain in eukaryotic cells serves as an oxygen sensor by releasing ROS in response to hypoxia. We speculate that the ROS produced under hypoxic/anoxic conditions in the GVC of corals after exposure to heat stress overwhelmed the first-line defense enzymes such as SOD and CAT, thus allowing lipid peroxidation. Deoxygenation is a major determinant of coral reef health (Altieri et al. 2017; Nelson and Altieri 2019; Hughes et al. 2020) and reflects the widespread decline in ocean oxygen that has occurred in recent decades (Oschlies et al. 2018). Low oxygen availability directly threatens coral survival through both lethal and sublethal stress responses (Johnson et al. 2017; Kealoha et al. 2020; Mallon et al. 2025). Further clarification is needed to better understand the effects of temperature-induced deoxygenation on coral microenvironments.

To conclude, our study provides the first evidence that thermal stress induces oxygen depletion and oxidative damage within the gastrovascular cavity and the gastrodermis of tropical corals. These local microenvironmental changes reflect the conditions experienced by the coral host and its symbionts as temperatures rise, highlighting how local stress dynamics could eventually extend to affect the holobiont. These conditions can affect nutrient exchange, metabolic balance, and the stability of the symbiosis. Accordingly, microenvironmental dynamics should be interpreted as integrative indicators of *in-hospite* functioning, reflecting the actual response within compartments in which key metabolic exchanges and stress regulation take place. Changes in oxygen dynamics in the GVC and prelethal oxidative stress observed in the gastrodermis may also serve as early warning signals of holobiont destabilization before visible bleaching signs.

Our results highlight the complexity of coral responses to ongoing ocean warming and the importance of considering host-symbiont-microbe interactions in different compartments of the holobiont. However, we also note some limitations in the present study. While light intensity was kept stable in this experiment, the combination of heat and light stress is a significant contributor to oxidative stress. As discussed by Lesser (2024), heat stress alone generates relatively small ROS fluxes, and reactive nitrogen species (RNS) may play a more important role, particularly at low irradiance. Moreover, ROS can originate from multiple sources, so our focus on gastrodermal enzymes may have missed other primary sites of ROS generation, as our measurements were confined to a few microenvironments (GVC and external tissue surface) without evaluating other compartments or tissues, such as the ectoderm or mitochondria-rich host tissues. This emphasizes the importance of future studies that combine compartment-specific ROS measurements with biochemical analyses to fully understand oxidative stress responses in corals. Laboratory conditions cannot fully reproduce natural environmental variability, such as diurnal fluctuations in light and temperature, although the parameters used in this experiment were set within the range commonly applied in laboratory studies. Direct data on the composition and functional role of the microbial community is lacking, albeit the GVC microbiome likely modulates the observed responses (Bollati et al. 2024). We note that our results thus reflect short-term, compartment-specific responses rather than the complete scope of holobiont dynamics under environmental stress. Future studies should address these gaps by studying multiple holobiont compartments under different light and temperature conditions. This will help clarify how various stressors interact to influence coral physiology. To understand how the GVC microbiome influences oxygen dynamics, ROS and RNS fluxes, and holobiont resilience, it is essential to evaluate its composition and functional role. Combining measurements from specific compartments with holobiont-level physiology would provide a more comprehensive view of how corals

respond to thermal stress. Currently, few studies have systematically compared different microenvironments within the holobiont or examined how these compartments respond to environmental stress. Future research should focus on the characteristics of the GVC microbiome and other microenvironments under normal and combined stress conditions, as well as in light and dark, and on the role of microbial communities in supporting coral resilience. Moreover, to understand the complexities of coral oxidative responses, it is essential to have a better understanding of the time-dependent dynamics of oxygen production and consumption, as well as the generation of hydrogen peroxide under thermal stress, and how those dynamics relate to other physiological stress markers. Such an integrative approach will be pivotal to enhancing our knowledge of coral response and resilience under climate change.

Supplementary Information The online version contains supplementary material available at https://doi.org/10.1007/s00227-025-04775-5.

Acknowledgments We thank Dirk De Beer and Gaby Eickert (Max Planck Institute for Marine Microbiology) for teaching QZ how to make and use hydrogen peroxide microsensors. This research was funded by grants from the European Union (VV: Traineeship ERASMUS+ 2023/2024 Agreement n. 33; WD: Grant Agreement n. 101062810, MedCorP), the Gordon and Betty Moore Foundation (MK; grant n. GBMF9206; https://doi.org/10.37807/GBMF9206), and a PhD scholarship from the China Scholarship Council (QZ). The funders had no role in study design, data collection and analysis, decision to publish, or preparation of the manuscript. Thanks to Biorender.com and DeepL.com for graphic and linguistic support.

Author contributions Conceptualization: V.V., W.D., M.K.; Methodology: V.V., W.D., M.K., Q.Z., E.M., D.S.; Investigation: V.V., Q.Z., E.M.; Data curation: V.V., W.D., G.M.; Formal analysis: V.V., W.D., G.M.; Resources: W.D., D.S., M.R., M.K.; Supervision: W.D., D.S., M.R., M.K.; Writing – original draft: V.V.; Writing – review & editing: All authors.

Funding Open access funding provided by Università degli Studi di Trieste within the CRUI-CARE Agreement. This research was funded by grants from the European Union (VV: Traineeship ERASMUS+2023/2024 Agreement n. 33; WD: Grant Agreement n. 101062810, MedCorP), the Gordon and Betty Moore Foundation (MK; grant n. GBMF9206; https://doi.org/10.37807/GBMF9206), and a PhD scholarship from the China Scholarship Council (QZ). The funders had no role in study design, data collection and analysis, decision to publish, or preparation of the manuscript.

Data availability The dataset and R codes for statistical analysis and plots presented in this study are available in the online repository Zenodo: https://doi.org/10.5281/zenodo.14967903 (DOI: https://zenodo.org/records/14967904).

Declarations

Conflict of interest The authors declare no relevant financial or non-financial conflicts of interest to disclose.

Ethical approval This study did not involve human participants or vertebrate animals, and all research activities complied with international guidelines for the ethical use of marine organisms.

References

Aebi H (1984) [13] Catalase *in vitro*. Methods in Enzymology. Academic Press, pp 121–126

Agostini S, Suzuki Y, Higuchi T, Casareto BE, Yoshinaga K, Nakano Y, Fujimura H (2012) Biological and chemical characteristics of the coral gastric cavity. Coral Reefs 31:147–156. https://doi.org/10.1007/s00338-011-0831-6

Agostini S, Fujimura H, Higuchi T, Yuyama I, Casareto BE, Suzuki Y, Nakano Y (2013) The effects of thermal and high-CO_2 stresses on the metabolism and surrounding microenvironment of the coral *Galaxea fascicularis*. CR Biol 336:384–391. https://doi.org/10.1016/j.crvi.2013.07.003

Al-Horani FA, Ferdelman T, Al-Moghrabi SM, de Beer D (2005) Spatial distribution of calcification and photosynthesis in the scleractinian coral *Galaxea fascicularis*. Coral Reefs 24:173–180. https://doi.org/10.1007/s00338-004-0461-3

Altieri AH, Harrison SB, Seemann J, Collin R, Diaz RJ, Knowlton N (2017) Tropical dead zones and mass mortalities on coral reefs. Proc Natl Acad Sci 114:3660–3665. https://doi.org/10.1073/pnas.1621517114

Apprill A (2025) Bacteria and archaea within coral reef ecosystems. In: Peixoto RS, Voolstra CR (eds) Coral reef microbiome. Springer Nature Switzerland, Cham, pp 25–39

Armoza-Zvuloni R, Schneider A, Sher D, Shaked Y (2016) Rapid Hydrogen Peroxide release from the coral *Stylophora pistillata* during feeding and in response to chemical and physical stimuli. Sci Rep 6:21000. https://doi.org/10.1038/srep21000

Baird AH, Bhagooli R, Ralph PJ, Takahashi S (2009) Coral bleaching: the role of the host. Trends Ecol Evol 24:16–20. https://doi.org/10.1016/j.tree.2008.09.005

Bartoń K (2020) "Package MuMIn - Multi-Model Inference."

Ben-Zvi O, Roberts P, Ratelle D, Snider J, Lertvilai P, Wangpraseurt D, Deheyn DD, Smith JE, Jaffe JS (2025) The benthic underwater microscope imaging PAM (BUMP): a non-invasive tool for in situ assessment of microstructure and photosynthetic efficiency. Methods Ecol Evol 16:1617–1624. https://doi.org/10.1111/2041-210X.70078

Berteotti S (2015) Non-Photochemical Quenching (NPQ) and biomass production in microalgae

Bhagooli R, Hidaka M (2003) Comparison of stress susceptibility of *in hospite* and isolated zooxanthellae among five coral species. J Exp Mar Biol Ecol 291:181–197. https://doi.org/10.1016/S0022-0981(03)00121-7

Bhagooli R, Hidaka M (2004) Release of zooxanthellae with intact photosynthetic activity by the coral *Galaxea fascicularis* in

response to high temperature stress. Mar Biol 145:329–337. https://doi.org/10.1007/s00227-004-1309-7

Bollati E, Hughes D, Suggett D, Raina J-B, Kühl M (2024) Microscale sampling of the coral gastrovascular cavity reveals a gut-like microbial community. Anim Microbiome. https://doi.org/10.1186/s42523-024-00341-4

Bove CB, Whitehead RF, Szmant AM (2020) Responses of coral gastrovascular cavity pH during light and dark incubations to reduced seawater pH suggest species-specific responses to the effects of ocean acidification on calcification. Coral Reefs 39:1675–1691. https://doi.org/10.1007/s00338-020-01995-7

Bradford MM (1976) A rapid and sensitive method for the quantitation of microgram quantities of protein utilizing the principle of protein-dye binding. Anal Biochem 72:248–254. https://doi.org/10.1006/abio.1976.9999

Brodersen KE, Lichtenberg M, Ralph PJ, Kühl M, Wangpraseurt D (2014) Radiative energy budget reveals high photosynthetic efficiency in symbiont-bearing corals. J R Soc Interface 11:20130997. https://doi.org/10.1098/rsif.2013.0997

Brown BE, Ambarsari I, Warner ME, Fitt WK, Dunne RP, Gibb SW, Cummings DG (1999) Diurnal changes in photochemical efficiency and xanthophyll concentrations in shallow water reef corals : evidence for photoinhibition and photoprotection. Coral Reefs 18:99–105. https://doi.org/10.1007/s003380050163

Buck JM, Sherman J, Bártulos CR, Serif M, Halder M, Henkel J, Falciatore A, Lavaud J, Gorbunov MY, Kroth PG, Falkowski PG, Lepetit B (2019) Lhcx proteins provide photoprotection via thermal dissipation of absorbed light in the diatom *Phaeodactylum tricornutum*. Nat Commun 10:4167. https://doi.org/10.1038/s41467-019-12043-6

Chandel NS, Maltepe E, Goldwasser E, Mathieu CE, Simon MC, Schumacker PT (1998) Mitochondrial reactive oxygen species trigger hypoxia-induced transcription. Proc Natl Acad Sci USA 95:11715–11720. https://doi.org/10.1073/pnas.95.20.11715

Cheng M, Luo Y, Yu X-L, Huang L-T, Lian J-S, Huang H (2024) Effects of elevated temperature and copper exposure on the physiological state of the coral *Galaxea fascicularis*. Mar Environ Res 193:106218. https://doi.org/10.1016/j.marenvres.2023.106218

Coles SL, Jokiel PL (1977) Effects of temperature on photosynthesis and respiration in hermatypic corals. Mar Biol 43:209–216. https://doi.org/10.1007/BF00402313

Cooper TF, Ulstrup KE, Dandan SS, Heyward AJ, Kühl M, Muirhead A, O'Leary RA, Ziersen BEF, Van Oppen MJH (2011) Niche specialization of reef-building corals in the mesophotic zone: metabolic trade-offs between divergent *Symbiodinium* types. Proc R Soc B Biol Sci 278:1840–1850. https://doi.org/10.1098/rspb.2010.2321

Deleja M, Paula JR, Repolho T, Franzitta M, Baptista M, Lopes V, Simão S, Fonseca VF, Duarte B, Rosa R (2022) Effects of hypoxia on coral photobiology and oxidative stress. Biology 11:1068. https://doi.org/10.3390/biology11071068

Dellisanti W, Zhang Q, Ferrier-Pagès C, Kühl M (2024) Contrasting effects of increasing dissolved iron on photosynthesis and O_2 availability in the gastric cavity of two Mediterranean corals. PeerJ 12:e17259. https://doi.org/10.7717/peerj.17259

Derks A, Schaven K, Bruce D (2015) Diverse mechanisms for photoprotection in photosynthesis. Dynamic regulation of photosystem II excitation in response to rapid environmental change. Biochim Biophys Acta BBA - Bioenerg 1847:468–485. https://doi.org/10.1016/j.bbabio.2015.02.008

Dias M, Ferreira A, Gouveia R, Madeira C, Jogee N, Cabral H, Diniz M, Vinagre C (2019a) Long-term exposure to increasing temperatures on scleractinian coral fragments reveals oxidative stress. Mar Environ Res 150:104758. https://doi.org/10.1016/j.marenvres.2019.104758

Dias M, Madeira C, Jogee N, Ferreira A, Gouveia R, Cabral H, Diniz M, Vinagre C (2019b) Oxidative stress on scleractinian coral fragments following exposure to high temperature and low salinity. Ecol Indic 107:105586. https://doi.org/10.1016/j.ecolind.2019.105586

Dias M, Madeira C, Jogee N, Ferreira A, Gouveia R, Cabral H, Diniz M, Vinagre C (2020) Integrative indices for health assessment in reef corals under thermal stress. Ecol Indic 113:106230. https://doi.org/10.1016/j.ecolind.2020.106230

Diaz JM, Hansel CM, Apprill A, Brighi C, Zhang T, Weber L, McNally S, Xun L (2016) Species-specific control of external superoxide levels by the coral holobiont during a natural bleaching event. Nat Commun 7:13801. https://doi.org/10.1038/ncomms13801

Doering T, Maire J, Chan WY, Perez-Gonzalez A, Meyers L, Sakamoto R, Buthgamuwa I, Blackall LL, van Oppen MJH (2023) Comparing the role of ROS and RNS in the thermal stress response of two cnidarian models, *Exaiptasia diaphana* and *Galaxea fascicularis*. Antioxidants 12:1057. https://doi.org/10.3390/antiox12051057

Downs CA, Fauth JE, Halas JC, Dustan P, Bemiss J, Woodley CM (2002) Oxidative stress and seasonal coral bleaching. Free Radic Biol Med 33:533–543. https://doi.org/10.1016/S0891-5849(02)00907-3

Duarte CM (2000) Marine biodiversity and ecosystem services: an elusive link. J Exp Mar Biol Ecol 250:117–131. https://doi.org/10.1016/S0022-0981(00)00194-5

Dunn SR, Schnitzler CE, Weis VM (2007) Apoptosis and autophagy as mechanisms of dinoflagellate symbiont release during cnidarian bleaching: every which way you lose. Proc R Soc B Biol Sci 274:3079–3085. https://doi.org/10.1098/rspb.2007.0711

Ferrario F, Beck MW, Storlazzi CD, Micheli F, Shepard CC, Airoldi L (2014) The effectiveness of coral reefs for coastal hazard risk reduction and adaptation. Nat Commun 5:1–9

Foyer CH, Hanke G (2022) ROS production and signalling in chloroplasts: cornerstones and evolving concepts. Plant J 111:642–661. https://doi.org/10.1111/tpj.15856

Franklin LA, Seaton GGR, Lovelock CE, Larkum AWD (1996) Photoinhibition of photosynthesis on a coral reef. Plant Cell Environ 19:825–836. https://doi.org/10.1111/j.1365-3040.1996.tb00419.x

Gardner SG, Raina J-B, Nitschke MR, Nielsen DA, Stat M, Motti CA, Ralph PJ, Petrou K (2017) A multi-trait systems approach reveals a response cascade to bleaching in corals. BMC Biol 15:117. https://doi.org/10.1186/s12915-017-0459-2

Gaschler MM, Stockwell BR (2017) Lipid peroxidation in cell death. Biochem Biophys Res Commun 482:419–425. https://doi.org/10.1016/j.bbrc.2016.10.086

Gattuso J-P, Magnan A, Billé R, Cheung WWL, Howes EL, Joos F, Allemand D, Bopp L, Cooley SR, Eakin CM, Hoegh-Guldberg O, Kelly RP, Pörtner H-O, Rogers AD, Baxter JM, Laffoley D, Osborn D, Rankovic A, Rochette J, Sumaila UR, Treyer S, Turley C (2015) Contrasting futures for ocean and society from different anthropogenic CO_2 emissions scenarios. Science 349:aac4722. https://doi.org/10.1126/science.aac4722

Gérard-Monnier D, Erdelmeier I, Régnard K, Moze-Henry N, Yadan JC, Chaudière J (1998) Reactions of 1-methyl-2-phenylindole with malondialdehyde and 4-hydroxyalkenals. Analytical applications to a colorimetric assay of lipid peroxidation. Chem Res Toxicol 11:1176–1183. https://doi.org/10.1021/tx9701790

Golden CD, Allison EH, Cheung WWL, Dey MM, Halpern BS, McCauley DJ, Smith M, Vaitla B, Zeller D, Myers SS (2016) Nutrition: fall in fish catch threatens human health. Nature 534:317–320. https://doi.org/10.1038/534317a

Gorbunov MY, Kolber ZS, Lesser MP, Falkowski PG (2001) Photosynthesis and photoprotection in symbiotic corals. Limnol Oceanogr 46:75–85. https://doi.org/10.4319/lo.2001.46.1.0075

Goulet TL, Erill I, Ascunce MS, Finley SJ, Javan GT (2020) Conceptualization of the holobiont paradigm as it pertains to corals. Front Physiol. https://doi.org/10.3389/fphys.2020.566968

Grabb KC, Kapit J, Wankel SD, Manganini K, Apprill A, Armenteros M, Hansel CM (2019) Development of a handheld submersible chemiluminescent sensor: quantification of superoxide at coral surfaces. Environ Sci Technol 53:13850–13858. https://doi.org/10.1021/acs.est.9b04022

Grottoli AG, Toonen RJ, van Woesik R, Vega Thurber R, Warner ME, McLachlan RH, Price JT, Bahr KD, Baums IB, Castillo KD, Coffroth MA, Cunning R, Dobson KL, Donahue MJ, Hench JL, Iglesias-Prieto R, Kemp DW, Kenkel CD, Kline DI, Kuffner IB, Matthews JL, Mayfield AB, Padilla-Gamiño JL, Palumbi S, Voolstra CR, Weis VM, Wu HC (2021) Increasing comparability among coral bleaching experiments. Ecol Appl 31:e02262. https://doi.org/10.1002/eap.2262

Guzy RD, Schumacker PT (2006) Oxygen sensing by mitochondria at complex III: the paradox of increased reactive oxygen species during hypoxia. Exp Physiol 91:807–819. https://doi.org/10.1113/expphysiol.2006.033506

Haas AF, Nelson CE, Kelly LW, Carlson CA, Rohwer F, Leichter JJ, Wyatt A, Smith JE (2011) Effects of coral reef benthic primary producers on dissolved organic carbon and microbial activity. PLoS ONE 6:e27973. https://doi.org/10.1371/journal.pone.0027973

Hakim JA, Koo H, Dennis LN, Kumar R, Ptacek T, Morrow CD, Lefkowitz EJ, Powell ML, Bej AK, Watts SA (2015) An abundance of Epsilonproteobacteria revealed in the gut microbiome of the laboratory cultured sea urchin, *Lytechinus variegatus*. Front Microbiol. https://doi.org/10.3389/fmicb.2015.01047

Hansel CM, Diaz JM (2021) Production of extracellular reactive oxygen species by marine biota. Annu Rev Mar Sci 13:177–200. https://doi.org/10.1146/annurev-marine-041320-102550

Harianto J, Carey N, Byrne M (2019) respR—an R package for the manipulation and analysis of respirometry data. Methods Ecol Evol 10:912–920. https://doi.org/10.1111/2041-210X.13162

Haro S, Brodersen KE, Bohórquez J, Papaspyrou S, Corzo A, Kühl M (2019) Radiative energy budgets in a microbial mat under different irradiance and tidal conditions. Microb Ecol 77:852–865. https://doi.org/10.1007/s00248-019-01350-6

Helgoe J, Davy SK, Weis VM, Rodriguez-Lanetty M (2024) Triggers, cascades, and endpoints: connecting the dots of coral bleaching mechanisms. Biol Rev 99:715–752. https://doi.org/10.1111/brv.13042

Hennige SJ, Suggett DJ, Warner ME, McDougall KE, Smith DJ (2009) Photobiology of *Symbiodinium* revisited: bio-physical and bio-optical signatures. Coral Reefs 28:179–195. https://doi.org/10.1007/s00338-008-0444-x

Higuchi T, Fujimura H, Arakaki T, Oomori T (2008) Activities of antioxidant enzymes (SOD and CAT) in the coral *Galaxea fascicularis* against increased hydrogen peroxide concentrations in seawater

Hill R, Larkum AWD, Frankart C, Kühl M, Ralph PJ (2004) Loss of functional photosystem II reaction centres in zooxanthellae of corals exposed to bleaching conditions: using fluorescence rise kinetics. Photosynth Res 82:59–72. https://doi.org/10.1023/B:PRES.0000040444.41179.09

Hill R, Frankart C, Ralph PJ (2005) Impact of bleaching conditions on the components of non-photochemical quenching in the zooxanthellae of a coral. J Exp Mar Biol Ecol 322:83–92. https://doi.org/10.1016/j.jembe.2005.02.011

Hoadley KD, Pettay DT, Grottoli AG, Cai W-J, Melman TF, Schoepf V, Hu X, Li Q, Xu H, Wang Y, Matsui Y, Baumann JH, Warner ME (2015) Physiological response to elevated temperature and pCO2 varies across four Pacific coral species: understanding the unique host+symbiont response. Sci Rep 5:18371. https://doi.org/10.1038/srep18371

Huang H, Dong Z, Huang L, Yang J, Di B, Li Y, Zhou G, Zhang C (2011) Latitudinal variation in algal symbionts within the scleractinian coral *Galaxea fascicularis* in the South China Sea. Mar Biol Res 7:208–211. https://doi.org/10.1080/17451000.2010.489616

Hughes DJ, Alderdice R, Cooney C, Kühl M, Pernice M, Voolstra CR, Suggett DJ (2020) Coral reef survival under accelerating ocean deoxygenation. Nat Clim Change 10:296–307. https://doi.org/10.1038/s41558-020-0737-9

Hughes DJ, Raina J-B, Nielsen DA, Suggett DJ, Kühl M (2022) Disentangling compartment functions in sessile marine invertebrates. Trends Ecol Evol 37:740–748. https://doi.org/10.1016/j.tree.2022.04.008

Isa V, Seveso D, Diamante L, Montalbetti E, Montano S, Gobbato J, Lavorano S, Galli P, Louis YD (2024) Physical and cellular impact of environmentally relevant microplastic exposure on thermally challenged *Pocillopora damicornis* (Cnidaria, Scleractinia). Sci Total Environ 918:170651. https://doi.org/10.1016/j.scitotenv.2024.170651

Isa V, Seveso D, Concari E, Becchi A, Saliu F, Lasagni M, Collina EM, Madaschi A, Lavorano S, Montano S, Louis YD, Montalbetti E (2025) Evidence of oxidative stress in the soft coral *Pinnigorgia flava* (Nutting, 1910) exposed to secondary plastic nanofibers and related leachates. Environ Pollut 366:125433. https://doi.org/10.1016/j.envpol.2024.125433

Jeffrey SW, Humphrey GF (1975) New spectrophotometric equations for determining chlorophylls *a*, *b*, *c*1 and *c*2 in higher plants, algae and natural phytoplankton. Biochem Physiol Pflanz 167:191–194. https://doi.org/10.1016/S0015-3796(17)30778-3

Johnson MD, Rodriguez L, Altieri A (2017) Shallow-water hypoxia and mass mortality on a Caribbean coral reef. Bull Mar Sci. https://doi.org/10.5343/bms.2017.1163

Jokic T, Borisov SM, Saf R, Nielsen DA, Kühl M, Klimant I (2012) Highly photostable near-infrared fluorescent pH indicators and sensors based on BF2-chelated tetraarylazadipyrromethene dyes. Anal Chem 84:6723–6730. https://doi.org/10.1021/ac3011796

Kahng SE, Odle E, Wakeman KC (2024) Coral geometry and why it matters. PeerJ 12:e17037. https://doi.org/10.7717/peerj.17037

Kealoha AK, Doyle SM, Shamberger KEF, Sylvan JB, Hetland RD, DiMarco SF (2020) Localized hypoxia may have caused coral reef mortality at the Flower Garden Banks. Coral Reefs 39:119–132. https://doi.org/10.1007/s00338-019-01883-9

Knowlton N, Rohwer F (2003) Multispecies microbial mutualisms on coral reefs: the host as a habitat. Am Nat 162:S51–S62. https://doi.org/10.1086/378684

Knowlton N, Brainard RE, Fisher R, Moews M, Plaisance L, Caley MJ (2010) Coral reefs biodiversity. In: McIntyre A (ed) Chater 4 Life in the world's oceans: diversity, distribution, and abundance. Wiley

Krämer WE, Caamaño-Ricken I, Richter C, Bischof K (2012) Dynamic regulation of photoprotection determines thermal tolerance of two phylotypes of *Symbiodinium* clade A at two photon fluence rates. Photochem Photobiol 88:398–413. https://doi.org/10.1111/j.1751-1097.2011.01048.x

Kühl M, Cohen Y, Dalsgaard T, Jørgensen B, Revsbech N (1995) Microenvironment and photosynthesis of zooxanthellae in scleractinian corals studied with microsensors for O2, pH and light. Mar Ecol Progr Series. 117:159–177

LaJeunesse TC, Parkinson JE, Gabrielson PW, Jeong HJ, Reimer JD, Voolstra CR, Santos SR (2018) Systematic revision of Symbiodiniaceae highlights the antiquity and diversity of coral endosymbionts. Curr Biol 28:2570-2580.e6. https://doi.org/10.1016/j.cub.2018.07.008

Lee Y, Kim M-S, Park JJC, Lee YH, Lee J-S (2022) Oxidative stress–mediated synergistic deleterious effects of nano- and microplastics in the hypoxia-conditioned marine rotifer *Brachionus plicatilis*. Mar Pollut Bull 181:113933. https://doi.org/10.1016/j.marpolbul.2022.113933

Lee Y, Byeon E, Kim D-H, Maszczyk P, Wang M, Wu RSS, Jeung H-D, Hwang U-K, Lee J-S (2023) Hypoxia in aquatic invertebrates: occurrence and phenotypic and molecular responses. Aquat Toxicol 263:106685. https://doi.org/10.1016/j.aquatox.2023.106685

Leggat WP, Camp EF, Suggett DJ, Heron SF, Fordyce AJ, Gardner S, Deakin L, Turner M, Beeching LJ, Kuzhiumparambil U, Eakin CM, Ainsworth TD (2019) Rapid coral decay is associated with marine heatwave mortality events on reefs. Curr Biol 29:2723-2730.e4. https://doi.org/10.1016/j.cub.2019.06.077

Lenth RV, Banfai B, Bolker B, Buerkner P, Giné-Vázquez I, Herve M, Jung M, Love J, Miguez F, Piaskowski J, Riebl H, Singmann H (2024) Emmeans: Estimated Marginal Means, aka Least-Squares Means

Lesser MP (2006) Oxidative stress in marine environments: biochemistry and physiological ecology. Annu Rev Physiol 68:253–278. https://doi.org/10.1146/annurev.physiol.68.040104.110001

Lesser MP (2011) Coral bleaching: causes and mechanisms. In: Dubinsky Z, Stambler N (eds) Coral reefs: an ecosystem in transition. Springer, Netherlands, Dordrecht, pp 405–419

Lesser MP (2024) Irradiance dependency of oxidative stress and coral bleaching. Coral Reefs 43:1393–1403. https://doi.org/10.1007/s00338-024-02545-1

Lesser MP, Weis VM, Patterson MR, Jokiel PL (1994) Effects of morphology and water motion on carbon delivery and productivity in the reef coral, *Pocillopora damicornis* (Linnaeus): diffusion barriers, inorganic carbon limitation, and biochemical plasticity. J Exp Mar Biol Ecol 178:153–179. https://doi.org/10.1016/0022-0981(94)90034-5

Liñán-Cabello MA, Flores-Ramírez LA, Zenteno-Savin T, Olguín-Monroy NO, Sosa-Avalos R, Patiño-Barragan M, Olivos-Ortiz A (2010) Seasonal changes of antioxidant and oxidative parameters in the coral *Pocillopora capitata* on the Pacific coast of Mexico. Mar Ecol 31:407–417. https://doi.org/10.1111/j.1439-0485.2009.00349.x

Linsmayer LB, Deheyn DD, Tomanek L, Tresguerres M (2020) Dynamic regulation of coral energy metabolism throughout the diel cycle. Sci Rep 10:19881. https://doi.org/10.1038/s41598-020-76828-2

Linsmayer LB, Noel SK, Leray M, Wangpraseurt D, Hassibi C, Kline DI, Tresguerres M (2024) Effects of bleaching on oxygen dynamics and energy metabolism of two Caribbean coral species. Sci Total Environ 919:170753. https://doi.org/10.1016/j.scitotenv.2024.170753

Long SP, Humphries S, Falkowski PG (1994) Photoinhibition of photosynthesis in nature. Annu Rev Plant Physiol Plant Mol Biol 45:633–662. https://doi.org/10.1146/annurev.pp.45.060194.003221

Mallon JE, Altieri AH, Cyronak T, Melendez-Declet CV, Valerie PJ, Johnson MD (2025) Sublethal changes to coral metabolism in response to deoxygenation. J Exp Biol Jeb. https://doi.org/10.1242/jeb.249638

Manning DWP, Rosemond AD, Gulis V, Benstead JP, Kominoski JS (2018) Nutrients and temperature additively increase stream microbial respiration. Glob Change Biol 24:e233–e247. https://doi.org/10.1111/gcb.13906

Marangoni LFdeB, Rottier C, Ferrier-Pagès C (2021) Symbiont regulation in *Stylophora pistillata* during cold stress: an acclimation mechanism against oxidative stress and severe bleaching. J Exp Biol 224:jeb235275. https://doi.org/10.1242/jeb.235275

Matsuda SB, Chakravarti LJ, Cunning R, Huffmyer AS, Nelson CE, Gates RD, van Oppen MJH (2022) Temperature-mediated acquisition of rare heterologous symbionts promotes survival of coral larvae under ocean warming. Glob Change Biol 28:2006–2025. https://doi.org/10.1111/gcb.16057

Mellin C, Brown S, Cantin N, Klein-Salas E, Mouillot D, Heron SF, Fordham DA (2024) Cumulative risk of future bleaching for the world's coral reefs. Sci Adv 10:eadn9660. https://doi.org/10.1126/sciadv.adn9660

Middlebrook R, Hoegh-Guldberg O, Leggat W (2008) The effect of thermal history on the susceptibility of reef-building corals to thermal stress. J Exp Biol 211:1050–1056. https://doi.org/10.1242/jeb.013284

Monserrat JM, Martínez PE, Geracitano LA, Lund Amado L, Martinez Gaspar Martins C, Lopes Leães Pinho G, Soares Chaves I, Ferreira-Cravo M, Ventura-Lima J, Bianchini A (2007) Pollution biomarkers in estuarine animals: critical review and new perspectives. Comp Biochem Physiol Toxicol Pharmacol CBP 146:221–234. https://doi.org/10.1016/j.cbpc.2006.08.012

Montalbetti E, Biscéré T, Ferrier-Pagès C, Houlbrèque F, Orlandi I, Forcella M, Galli P, Vai M, Seveso D (2021) Manganese benefits heat-stressed corals at the cellular level. Front Mar Sci. https://doi.org/10.3389/fmars.2021.681119

Montalbetti E, Cavallo S, Azzola A, Montano S, Galli P, Montefalcone M, Seveso D (2022a) Mucilage-induced necrosis reveals cellular oxidative stress in the Mediterranean gorgonian *Paramuricea clavata*. J Exp Mar Biol Ecol 559:151839. https://doi.org/10.1016/j.jembe.2022.151839

Montalbetti E, Isa V, Vencato S, Louis Y, Montano S, Lavorano S, Maggioni D, Galli P, Seveso D (2022b) Short-term microplastic exposure triggers cellular damage through oxidative stress in the soft coral *Coelogorgia palmosa*. Mar Biol Res 18:495–508. https://doi.org/10.1080/17451000.2022.2137199

Muscatine L, R. McCloskey L, E. Marian R (1981) Estimating the daily contribution of carbon from zooxanthellae to coral animal respiration1. Limnol Oceanogr 26:601–611. https://doi.org/10.4319/lo.1981.26.4.0601

Nelson HR, Altieri AH (2019) Oxygen: the universal currency on coral reefs. Coral Reefs 38:177–198. https://doi.org/10.1007/s00338-019-01765-0

Niyogi KK (1999) Photoprotection revisited: genetic and molecular approaches. Annu Rev Plant Physiol Plant Mol Biol 50:333–359. https://doi.org/10.1146/annurev.arplant.50.1.333

Oakley C, Davy S (2018) Cell biology of coral bleaching. pp 189–211

Oschlies A, Brandt P, Stramma L, Schmidtko S (2018) Drivers and mechanisms of ocean deoxygenation. Nat Geosci 11:467–473. https://doi.org/10.1038/s41561-018-0152-2

Ousley S, de Beer D, Bejarano S, Chennu A (2022) High-resolution dynamics of hydrogen peroxide on the surface of scleractinian corals in relation to photosynthesis and feeding. Front Mar Sci. https://doi.org/10.3389/fmars.2022.812839

Pachauri RK, Allen MR, Barros VR, Broome J, Cramer W, Christ R, Church JA, Clarke L, Dahe Q, Dasgupta P, Dubash NK, Edenhofer O, Elgizouli I, Field CB, Forster P, Friedlingstein P, Fuglestvedt J, Gomez-Echeverri L, Hallegatte S, Hegerl G, Howden M, Jiang K, Jimenez Cisneroz B, Kattsov V, Lee H, Mach KJ, Marotzke J, Mastrandrea MD, Meyer L, Minx J, Mulugetta Y, O'Brien K, Oppenheimer M, Pereira JJ, Pichs-Madruga R, Plattner G-K, Pörtner H-O, Power SB, Preston B, Ravindranath NH, Reisinger A, Riahi K, Rusticucci M, Scholes R, Seyboth K, Sokona Y, Stavins R, Stocker TF, Tschakert P, van Vuuren D, van Ypserle J-P (2014) Climate Change 2014: Synthesis Report. Contribution of Working Groups I, II and III to the Fifth Assessment Report of the Intergovernmental Panel on Climate Change. IPCC, Geneva, Switzerland

Pacherres CO, Ahmerkamp S, Koren K, Richter C, Holtappels M (2022) Ciliary flows in corals ventilate target areas of high photosynthetic oxygen production. Curr Biol 32:4150-4158.e3. https://doi.org/10.1016/j.cub.2022.07.071

Parkinson JE, Peixoto RS, Voolstra CR (2025) Symbiodiniaceae. In: Peixoto RS, Voolstra CR (eds) Coral reef microbiome. Springer Nature Switzerland, Cham, pp 9–23

Posit team (2025) RStudio: integrated development environment for R (2025.05.0+496. In: Posit. https://posit.co/download/rstudio-desktop/. Accessed 19 June 2025

Puntin G, Craggs J, Hayden R, Engelhardt KE, McIlroy S, Sweet M, Baker DM, Ziegler M (2023) The reef-building coral *Galaxea fascicularis*: a new model system for coral symbiosis research. Coral Reefs 42:239–252. https://doi.org/10.1007/s00338-022-02334-8

R Core Team (2024) R: A language and environment for statistical computing. R Foundation for Statistical Computing, Vienna, Austria

Rädecker N, Pogoreutz C, Voolstra CR, Wiedenmann J, Wild C (2015) Nitrogen cycling in corals: the key to understanding holobiont functioning? Trends Microbiol 23:490–497. https://doi.org/10.1016/j.tim.2015.03.008

Raijmakers JR (2024) Long exposure of the indo-pacific coral caulastrea furcata to presumed sublethal temperatures. MSc thesis

Ralph PJ, Schreiber U, Gademann R, Kühl M, Larkum AWD (2005) Coral photobiology studied with a new imaging pulse amplitude modulated fluorometer. J Phycol 41:335–342. https://doi.org/10.1111/j.1529-8817.2005.04034.x

Riedel TE, Berelson WM, Nealson KH, Finkel SE (2013) Oxygen consumption rates of bacteria under nutrient-limited conditions. Appl Environ Microbiol 79:4921–4931. https://doi.org/10.1128/AEM.00756-13

Robison JD, Warner ME (2006) Differential impacts of photoacclimation and thermal stress on the photobiology of four different phylotypes of Symbiodinium (pyrrhophyta). J Phycol 42:568–579. https://doi.org/10.1111/j.1529-8817.2006.00232.x

Rohwer F, Seguritan V, Azam F, Knowlton N (2002) Diversity and distribution of coral-associated bacteria. Mar Ecol Prog Ser 243:1–10. https://doi.org/10.3354/meps243001

Rosenberg E, Kellogg CA, Rohwer F (2007) Coral microbiology. Oceanography 20:146–154

Roth MS (2014) The engine of the reef: photobiology of the coral–algal symbiosis. Front Microbiol 5:422. https://doi.org/10.3389/fmicb.2014.00422

Saragosti E, Tchernov D, Katsir A, Shaked Y (2010) Extracellular production and degradation of superoxide in the coral *Stylophora pistillata* and cultured *Symbiodinium*. PLoS ONE 5:e12508. https://doi.org/10.1371/journal.pone.0012508

Sawall Y, Bakker R, Padillo-Anthemides NE, Adamson N (2025) Diurnal pattern of respiration in corals and algae and its implications for gross primary production quantification. PLoS ONE 20:e0326146. https://doi.org/10.1371/journal.pone.0326146

Schlotheuber M, Voolstra CR, de Beer D, Camp EF, Klatt JM, Ghilardi M, Neumüller K, Ousley S, Bejarano S (2024) High temporal resolution of hydrogen peroxide (H_2O_2) dynamics during heat stress does not support a causative role in coral bleaching. Coral Reefs 43:119–133. https://doi.org/10.1007/s00338-023-02448-7

Schoepf V, Cornwall C, Gillmann S, Carrion S, Alessi C, Comeau S, McCulloch M (2018) Impacts of coral bleaching on pH and oxygen gradients across the coral concentration boundary layer: a microsensor study. Coral Reefs. https://doi.org/10.1007/s00338-018-1726-6

Schreiber U (2004) Pulse-amplitude-modulation (PAM) fluorometry and saturation pulse method: an overview. In: Papageorgiou GC, Govindjee A (eds) Chlorophyll a fluorescence: a signature of photosynthesis. Springer, Netherlands, Dordrecht, pp 279–319

Schutter M, Van der Ven R, Janse M, Verreth J, Wijffels R, Osinga R (2012) Light intensity, photoperiod duration, daily light flux and coral growth of *Galaxea fascicularis* in an aquarium setting: a matter of photons? J Mar Biol Assoc U K 92:703–712. https://doi.org/10.1017/S0025315411000920

Shashar N, Cohen Y, Loya Y (1993) Extreme diel fluctuations of oxygen in diffusive boundary layers surrounding stony corals. Biol Bull. https://doi.org/10.2307/1542485

Shashar N, Kinane S, Jokiel PL, Patterson MR (1996) Hydromechanical boundary layers over a coral reef. J Exp Mar Biol Ecol 199:17–28. https://doi.org/10.1016/0022-0981(95)00156-5

Sobha TR, Vibija CP, Fahima P (2023) Coral reef: a hot spot of marine biodiversity. In: Sukumaran ST, Keerthi TR (eds) Conservation and sustainable utilization of bioresources. Springer Nature, Singapore, pp 171–194

Stanley G Jr, Swart P (1995) Evolution of the coral-zooxanthellae symbiosis during the Triassic: a geochemical approach. Paleobiology 21:179–199. https://doi.org/10.1017/S0094837300013191

Sully S, Hodgson G, van Woesik R (2022) Present and future bright and dark spots for coral reefs through climate change. Glob Change Biol 28:4509–4522. https://doi.org/10.1111/gcb.16083

Szabó M, Larkum A, Vass I (2020) A review: the role of reactive oxygen species in mass coral bleaching. pp 459–488

Tansik AL, Fitt WK, Hopkinson BM (2017) Inorganic carbon is scarce for symbionts in scleractinian corals. Limnol Oceanogr 62:2045–2055. https://doi.org/10.1002/lno.10550

Thomas FIM, Atkinson MJ (1997) Ammonium uptake by coral reefs: effects of water velocity and surface roughness on mass transfer. Limnol Oceanogr 42:81–88. https://doi.org/10.4319/lo.1997.42.1.0081

Torres AF, Valino DAM, Ravago-Gotanco R (2021) Zooxanthellae diversity and coral-symbiont associations in the Philippine Archipelago: specificity and adaptability across thermal gradients. Front Mar Sci. https://doi.org/10.3389/fmars.2021.731023

Ulstrup K, Berkelmans R, Ralph P, Van Oppen M (2006) Variation in bleaching sensitivity of two coral species across a latitudinal gradient on the Great Barrier Reef: the role of zooxanthellae. Mar Ecol Prog Ser 314:135–148. https://doi.org/10.3354/meps314135

van Oppen MJH, Medina M (2020) Coral evolutionary responses to microbial symbioses. Philos Trans R Soc Lond B Biol Sci 375:20190591. https://doi.org/10.1098/rstb.2019.0591

van Oppen MJH, Raina J-B (2023) Coral holobiont research needs spatial analyses at the microbial scale. Environ Microbiol 25:179–183. https://doi.org/10.1111/1462-2920.16237

van Hooidonk R, Maynard JA, Manzello D, Planes S (2014) Opposite latitudinal gradients in projected ocean acidification and bleaching impacts on coral reefs. Glob Change Biol 20:103–112. https://doi.org/10.1111/gcb.12394

van Woesik R, Shlesinger T, Grottoli AG, Toonen RJ, Vega Thurber R, Warner ME, Marie Hulver A, Chapron L, McLachlan RH, Albright R, Crandall E, DeCarlo TM, Donovan MK, Eirin-Lopez J, Harrison HB, Heron SF, Huang D, Humanes A, Krueger T, Madin JS, Manzello D, McManus LC, Matz M, Muller EM, Rodriguez-Lanetty M, Vega-Rodriguez M, Voolstra CR, Zaneveld J (2022) Coral-bleaching responses to climate change across biological scales. Glob Change Biol 28:4229–4250. https://doi.org/10.1111/gcb.16192

Wagner D, Friedlander AM, Pyle RL, Brooks CM, Gjerde KM, Wilhelm T (2020) Coral reefs of the High Seas: hidden biodiversity hotspots in need of protection. Front Mar Sci. https://doi.org/10.3389/fmars.2020.567428

Wang X, Zhang T, Zhang Q, Xue R, Qu Y, Wang Q, Dong Z, Zhao J (2022) Different patterns of hypoxia aggravate the toxicity of polystyrene nanoplastics in the mussels *Mytilus galloprovincialis*: environmental risk assessment of plastics under global

climate change. Sci Total Environ 818:151818. https://doi.org/10.1016/j.scitotenv.2021.151818

Wang C, Zheng X, Kvitt H, Sheng H, Sun D, Niu G, Tchernov D, Shi T (2023) Lineage-specific symbionts mediate differential coral responses to thermal stress. Microbiome 11:211. https://doi.org/10.1186/s40168-023-01653-4

Warner ME, Berry-Lowe S (2006) Differential xanthophyll cycling and photochemical activity in symbiotic dinoflagellates in multiple locations of three species of Caribbean coral. J Exp Mar Biol Ecol 339:86–95. https://doi.org/10.1016/j.jembe.2006.07.011

Warner ME, Fitt WK, Schmidt GW (1996) The effects of elevated temperature on the photosynthetic efficiency of zooxanthellae *in hospite* from four different species of reef coral: a novel approach. Plant Cell Environ 19:291–299. https://doi.org/10.1111/j.1365-3040.1996.tb00251.x

Warner M, Chilcoat G, McFarland F, Fitt W (2002) Seasonal fluctuations in the photosynthetic capacity of photosystem II in symbiotic dinoflagellates in the Caribbean reef-building coral *Montastraea*. Mar Biol 141:31–38. https://doi.org/10.1007/s00227-002-0807-8

Weis VM (2008) Cellular mechanisms of Cnidarian bleaching: stress causes the collapse of symbiosis. J Exp Biol 211:3059–3066. https://doi.org/10.1242/jeb.009597

Weis VM (2019) Cell biology of coral symbiosis: foundational study can inform solutions to the coral reef crisis. Integr Comp Biol 59:845–855. https://doi.org/10.1093/icb/icz067

Wickham H (2016) ggplot2. Springer International Publishing, Cham

Woodhead AJ, Hicks CC, Norström AV, Williams GJ, Graham NAJ (2019) Coral reef ecosystem services in the Anthropocene. Funct Ecol 33:1023–1034. https://doi.org/10.1111/1365-2435.13331

Yellowlees D, Rees TAV, Leggat W (2008) Metabolic interactions between algal symbionts and invertebrate hosts. Plant Cell Environ 31:679–694. https://doi.org/10.1111/j.1365-3040.2008.01802.x